Byrne MJ, Lees NR, Han LC, van der Kamp MW, Mulholland AJ, Stach JEM, Willis CL, Race PR.

The Catalytic Mechanism of a Natural Diels-Alderase Revealed in Molecular Detail.

***Journal of the American Chemical Society* 2016, 138(19), 6095-6098**

The catalytic mechanism of a natural Diels-Alderase revealed in molecular detail

Matthew J. Byrne,[†,‡] Nicholas R. Lees,[§] Li-Chen Han,[‡,§] Marc W. van der Kamp,[†,‡,§] Adrian J. Mulholland,[‡,§] James E.M. Stach,[//,⊥] Christine L. Willis,[‡,§] and Paul R. Race[*,†,‡]

[†]*School of Biochemistry, Biomedical Sciences Building, University Walk, University of Bristol, BS8 1TD, UK.*
[‡]*BrisSynBio Synthetic Biology Research Centre, Life Sciences Building, Tyndall Avenue, University of Bristol, BS8 1TQ, UK.*
[§]*School of Chemistry, Cantock's Close, University of Bristol, BS8 1TS, UK.*
[//]*School of Biology, Ridley Building, Newcastle University, NE1 7RU, UK.*
[⊥]*Centre for Synthetic Biology and the Bioeconomy, Baddiley-Clark Building, Newcastle University, NE2 4AX, UK.*

Supporting Information Placeholder

ABSTRACT: The Diels-Alder reaction, a [4+2] cycloaddition of a conjugated diene to a dienophile, is one of the most powerful reactions in synthetic chemistry. Biocatalysts capable of unlocking new and efficient Diels-Alder reactions would have major impact. Here we present a molecular-level description of the reaction mechanism of the spirotetronate cyclase AbyU, an enzyme shown here to be a *bona fide* natural Diels-Alderase. Using enzyme assays, X-ray crystal structures and simulations of the reaction in the enzyme, we reveal how linear substrate chains are contorted within the AbyU active site to facilitate a transannular pericyclic reaction. This study provides compelling evidence for the existence of a natural enzyme evolved to catalyze a Diels-Alder reaction, and shows how catalysis is achieved.

The Diels-Alder reaction is a [4+2] cycloaddition that involves the reorganization of a six-electron system to form a cyclohexene.[1] This transformation is of major synthetic value for the preparation of substituted six-membered rings with the creation of up to four new stereocenters.[2–5] Development of protein catalysts for these reactions is a major goal in biocatalysis, and would potentially enable new, efficient and 'green' synthetic routes to a wide variety of valuable bioactive compounds. Whilst a small number of natural enzymes have been shown to be capable of catalyzing [4+2] cycloaddition reactions[6–13] the molecular details of how these transformations are achieved, and whether they do indeed proceed *via* a formal Diels-Alder route, remain unknown.[14–16] Detailed mechanistic studies of protein-catalyzed Diels-Alder reactions have to date been restricted to *de novo* designed enzymes and catalytic antibodies.[17,18] These valuable test subjects, however, exhibit poor catalytic efficiencies, limiting their value as biocatalysts.[19,20] Establishing whether natural enzymes have evolved Diels-Alderase activity, and in particular, how such catalysis is achieved at the molecular level, is crucial for the development of efficient protein Diels-Alder catalysts.[15-18,21]

We focus on the putative natural Diels-Alderase AbyU, from the abyssomicin C biosynthetic pathway. The spirotetronate antibiotic abyssomicin C (**1**), first isolated from the marine actinomycete *Verrucosispora maris* AB-18-032, is a potent inhibitor of bacterial folate metabolism effective against *Mycobacterium tuberculosis* and multi-drug resistant clinical isolates of *Staphylococcus aureus*.[22] The biosynthesis of this compound proceeds *via* the formation of a heterobicyclic ring system, comprising a tetronic acid ring (4-hydroxy-[5*H*]furan-2-one) spiro-linked to cyclohexene[23] (Figure 1). Formation of this carbocycle is postulated to occur *via* an enzyme-catalyzed intramolecular [4+2] cycloaddition between the exocyclic methylene group and conjugated diene of **4**.[24,25] This transformation could conceivably progress *via* a formal Diels-Alder reaction. Studies of enzymes from other spirotetronate biosynthetic pathways have demonstrated the presence of a stand-alone cyclase that facilitates [4+2] cycloaddition.[12,13] However, the molecular basis of how this reaction is performed and whether it does indeed progress *via* a concerted mechanism are unknown. Given that spirotetronate cyclases share no amino acid sequence identity to other putative natural Diels-Alderases,[4,6–13] it is likely that these enzymes represent a distinct protein scaffold in which a Diels-Alder reaction may take place.

An N-terminally hexa-histidine tagged variant of AbyU was recombinantly over-expressed in *E. coli* B834(DE3) cells and purified to homogeneity. Purified recombinant AbyU was found to be a homogeneous, dimeric species in solution, of >95% purity (Figure S1).

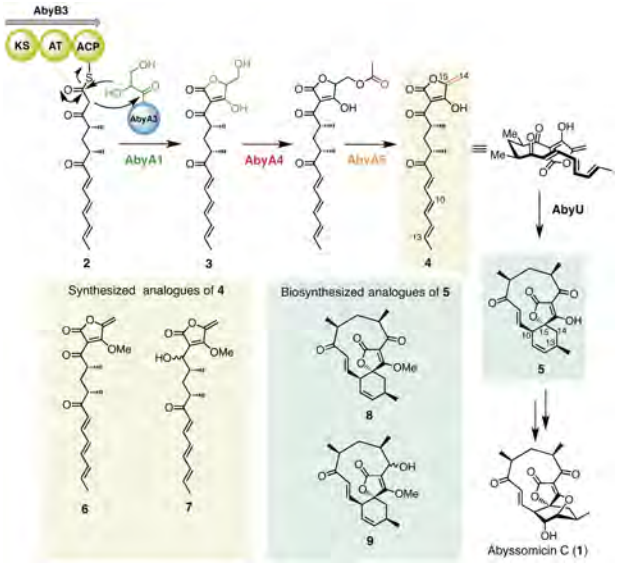

Figure 1. Proposed abyssomicin C biosynthetic pathway, synthetic substrate analogues (**6** and **7**) and biosynthesized spirotetronates (**8** and **9**). During the biosynthesis of abyssomicin C the heptaketide product **2** of the AbyB1-3 polyketide synthase is condensed with glycerate, presented on the free-standing acyl carrier protein AbyA3, to form a 5-membered ring in **3**. Acetylation of **3** followed by elimination, catalyzed by the AbyA4/AbyA5 enzyme couple, introduces the exocyclic methylene of **4**. Intramolecular [4+2] cycloaddition of **4** is catalyzed by AbyU and yields the spirotetronate abyssomicin C precursor **5**. Structural and functional studies of AbyU reported herein were conducted using substrate analogues **6** and **7**, which were enzymatically converted to **8** and **9** respectively.

Substrate **6,** an analogue of the proposed AbyU substrate **4** (Figure 1) was synthesized and incubated with AbyU for 30 mins at 25 °C. Analysis of the resulting reaction mixture by HPLC indicated that a single product had been formed with the same retention time as a standard of **8**, prepared by heating diketone **6** for 2 days in chloroform (Figure 2). The mass of this product (*m*/*z* = 367.53) and ^{1}H-NMR of the crude material were in accord with the spirocyclic product **8** (Figure S2 and SI). There was no evidence of cyclization occurring in control reactions lacking enzyme, or containing heat-denatured AbyU (Figure 2). Steady-state kinetic characterization of the AbyU catalyzed conversion of **6** to **8** gave k_{cat} = 564 ± 43 min^{-1}, K_m = 102 ± 17 μM and k_{cat}/K_m = 5.5 ± 0.2 min^{-1}μM^{-1}. This compares with a rate for the non-AbyU catalyzed reaction of k = 0.014 min^{-1}, consistent with a > 4 x 10^{4} fold enhancement in rate in the presence of enzyme (Figure S3). Whilst these data give compelling support for an AbyU mediated [4+2] cycloaddition, diketone **6** is known to slowly undergo a Diels-Alder reaction at room temperature (40% conversion after one week in chloroform[26] and Figure S3). To further explore the potential value of AbyU, a substrate less prone to undergo cyclization was investigated.

Since in general, electron-deficient dienophiles are favored in Diels-Alder reactions, a mixture of epimeric alcohols **7**, the synthetic precursor of diketone **6**, was selected. Neither incubation of **7** in aqueous buffer for 24 hrs, nor heating of **7** in chloroform for 2 days gave the cycloadduct **9**. In contrast, incubation of **7** with AbyU for 30 mins at 25 °C yielded two products (Figure 2) with the correct mass (*m*/*z*=369.63) for the epimeric cycloaddition products **9** (Figure S2), indicating that an intramolecular [4+2] cycloaddition had taken place. No synthetic standard of **9** was available for comparison. To circumvent this, the mixture of **9** from the AbyU-catalyzed reaction was purified by preparative TLC and oxidized using Dess-Martin periodinane, to yield a less polar product (Figure 2 and SI), which exhibited a retention profile, mass spectrum (*m*/*z*=367.53), and ^{1}H NMR data in accord with the synthetic spirotetronate **8**. No product was detected in control reactions with heat-denatured AbyU. Together, these data show that AbyU is capable of catalyzing [4+2] cycloaddition reactions, including one that cannot be readily achieved under standard conditions of prolonged heating.

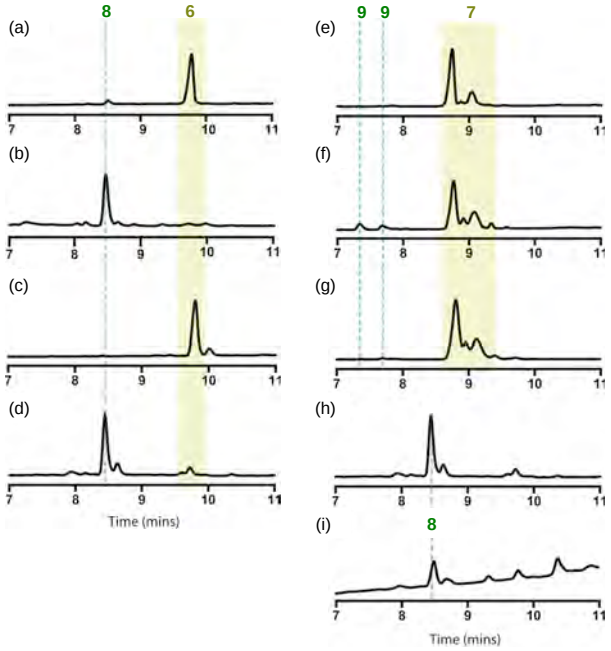

Figure 2. HPLC analysis demonstrating AbyU catalyzed [4+2] cycloaddition. Traces are shown for assay mixes comprising: (a), synthetic standard of diketone **6**; (b), **6** incubated with 280 μM AbyU; (c), **6** incubated with 280 μM heat denatured AbyU; (d), synthetic standard of Diels-Alder product **8**; (e), synthetic standard of diol **7** (as a mixture of epimeric alcohols); (f), **7** incubated with 280 μM AbyU; (g), **7** incubated with 280 μM heat denatured AbyU; (h), synthetic standard of Diels-Alder product **8**; (i), product from the purification of **9** isolated from (f) followed by oxidation using Dess-Martin periodinane to give **8**. Standard incubation conditions comprised 10 mM substrate with or without AbyU for 30 mins at 25 ^{o}C.

To analyze the molecular basis of the AbyU-catalyzed cycloaddition, we determined the crystal structure of the enzyme (Figure 3).

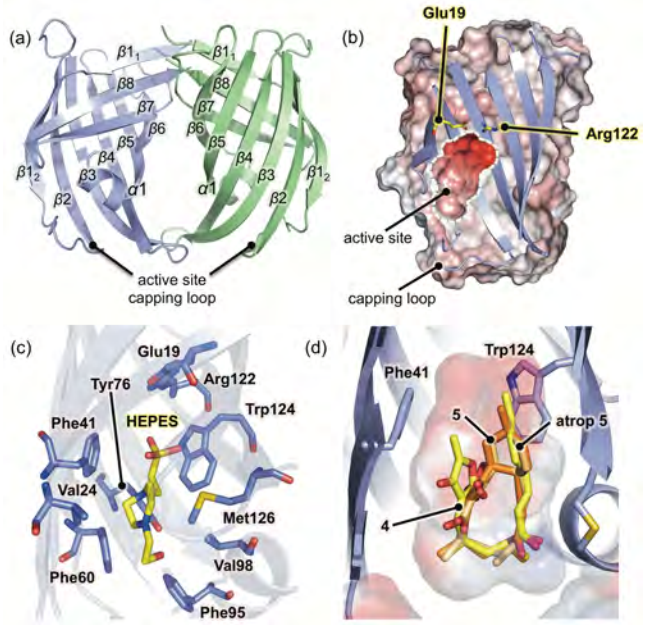

Figure 3. Crystal structure of AbyU and substrate binding mode. (a), Overall fold of the AbyU dimer. Individual monomers are colored blue and green respectively. (b), Cut-away view through crystal structure of AbyU, revealing the size and location of the enzyme active site. The protein is shown in space filling representation and is colored by electrostatic surface potential. The residues Glu19 and Arg122 are shown in stick format and colored by atom. (c), Detailed view of the AbyU active site highlighting key residues and bound molecule of HEPES. Coloring is by atom. (d), Superposition of the computationally predicted binding modes of **4**, **5** and the atropisomer of **5** within the active site of AbyU.

For the purposes of phase determination, a mutant of AbyU (AbyU_DM) was generated in which the residues Leu73 and Leu139 were replaced with selenomethionines, using methionine encoding codons (Figure S4). AbyU_DM was recombinantly over-expressed in *E. coli* and purified to homogeneity. As with AbyU, AbyU_DM was found to be dimeric in solution (Figure S1). The crystal structure of AbyU_DM was determined to 1.7 Å resolution using the single wavelength anomalous dispersion (SAD) method as applied to selenomethionine (SeMet) labeled crystals of AbyU_DM. This structure was subsequently used as a molecular replacement search model to elucidate the crystal structure of AbyU. The Cα RMSD between AbyU_DM and AbyU is 0.4 Å (Figure S5). Both unlabeled and SeMet labeled AbyU_DM catalyzed the conversion of **6** to **8** (Figure S6), confirming their catalytic competency.

AbyU is a homodimer comprised of two eight stranded anti-parallel β-barrels with (+1)8 topology (Figure 3). The central channel of each barrel is sealed at one end by a salt bridge formed by the side-chains of Glu19 and Arg122 and is capped at the other by a largely hydrophobic loop formed by the β1-β2 linker (residues Asp26-Gly36; Figure 3). Molecular dynamics simulations demonstrate the flexible nature of the capping loop and its ability to gate active site access (Figure S7). The central channel of the barrel forms an extended largely hydrophobic cavity of ~720 Å^3 that constitutes the active site of the enzyme, formed by the side chains of the residues Val21, Phe41, Phe60, Tyr76, Phe95, Tyr106, Trp124 and Met126 (Figure 3). Electron density corresponding to a single bound HEPES molecule is observed in the active sites of each of the 8 copies of AbyU and three of the four copies of AbyU_DM that comprise their respective asymmetric units (Figures 3 and S5).

AbyU's closest structural homolog is the allene oxide cyclase PpAOC2:[27] a more elaborated eight stranded barrel with a significantly different active site architecture (Figure S8). Comparison of the sequence of AbyU with those of other known spirotetronate cyclases reveals minimal sequence conservation (Figure S9), raising the intriguing possibility that mutation of the internal cavity of barrel-like structures may offer a route to generating enzymes capable of performing [4+2] cycloaddition reactions using a range of substrates.

To establish the catalytic mechanism of AbyU, we first investigated the binding mode of the substrate associated with the reaction. Docking of **4**, **5** and the atropisomer of **5** in the active site supports a binding mode where the substrate dienophile is positioned next to Phe41 and the diene close to Trp124 (Figures 3 and S10). In this binding mode, a hydrogen bond is formed between Tyr76 and the lactone carbonyl, which may contribute to substrate specificity. Binding is largely hydrophobic, with good steric complementarity between the enzyme and substrate. In the docked conformation of **4**, the C13-C14 and C10-C15 distances (bonds formed in the product) are 3.6 and 3.9 Å, respectively. This indicates that the enzyme active site accommodates the substrate in a potentially reactive Michaelis conformation. Molecular dynamics (MD) simulations of the enzyme with product **5** bound show that the binding mode obtained from docking is stable. Little structural change of the enzyme is required to accommodate the substrate; comparison of MD simulations of the *apo* and substrate-bound enzymes primarily show changes in the loop covering the active site cavity (residues 26-36), which becomes more ordered on substrate binding (Figure S7).

Quantum mechanics/molecular mechanics (QM/MM) molecular dynamics simulations, which incorporate the effects of the enzyme on the reaction[28], reveal that the reaction in the enzyme proceeds *via* a concerted, asynchronous Diels-Alder mechanism (Figures S10 and S11). They show that the substrate can react from the binding mode described above. The structural and

electronic properties of the transition state (Figures S10 and S11) indicate that AbyU is indeed a true Diels-Alderase. Free-energy profiles of the reaction were calculated at the SCC-DFTB/ff14SB QM/MM level, with the reaction simulated in the reverse direction, **5** to **4**. The active site is well organized to catalyze the reaction and the interactions noted above are maintained throughout. In the transition state, C13-C14 bond formation is more advanced than C10-C15 bond formation, which occurs predominantly on the downhill path to the product (Figure S10). Higher-level density functional theory calculations (M06-2X/6-31G(d,p)) confirm the identification of the transition state structure and the order of bond formation (Figure S11). Both levels of theory thus show that the [4+2] cycloaddition of **4** to **5** occurs *via* an asynchronous concerted Diels-Alder mechanism. The transition state structures calculated for the reaction of the isolated substrate are similar to those in the enzyme, which indicates that the primary catalytic function of the enzyme is to provide a preorganized active site that binds a reactive conformation of the substrate, from which the reaction can occur with a relatively low free energy barrier.

In summary, we report the structural and functional characterization of the spirotetronate cyclase AbyU, establishing the molecular basis of the [4+2] cycloaddition reaction catalyzed by this enzyme. AbyU is a co-factor independent, stand-alone Diels-Alderase with a low-molecular weight beta-barrel scaffold. The simplicity of this enzyme makes it a compelling and practical target for engineering. It has further been shown capable of accepting and acting upon non-natural substrates, including those that do not readily cyclize upon heating. This study presents unequivocal evidence of the existence of a natural enzyme capable of catalyzing a formal Diels-Alder reaction and paves the way for the exploitation of AbyU as a biocatalyst for industrial applications and the designed synthesis of novel bioactive compounds.

ASSOCIATED CONTENT

Supporting Information Available. Experimental procedures, Figures S1-S11, Table S1, compound spectra and supplementary references.

AUTHOR INFORMATION

Corresponding Author

*paul.race@bristol.ac.uk

Notes

The authors declare no competing financial interest. During review of this manuscript the crystal structure of the spirotetramate cyclase PyrI4 was published.[29]

ACKNOWLEDGMENTS

This work was supported by BBSRC and EPSRC through the BrisSynBio Synthetic Biology Research Centre (BB/L01386X/1), PhD studentships awarded to MJB (BBSRC, BB/D526037/1) and NRL (EPSRC, EP/G0367641/1 and GSK), and a BBSRC David Phillips Fellowship to MWvdK (BB/M026280/1). The authors thank Professors Tom Simpson FRS and Varinder Aggarwal FRS for fruitful discussions.

REFERENCES

(1) Diels, O.; Alder, K. *Justus Liebigs Ann. Chem.* **1928**, *460* (1), 98–122.
(2) Carruthers, W. Ed. *Cycloaddition Reactions in Organic Synthesis*; Elsevier, **1990**.
(3) Nicolaou, K. C.; Snyder, S. A.; Montagnon, T.; Vassilikogiannakis, G. *Angew. Chemie. Int. Ed.* **2002**, *41* (10), 1668–1698.
(4) Oikawa, H.; Katayama, K.; Suzuki, Y.; Ichihara, A. *J. Chem. Soc. Chem. Commun.* **1995**, *13*, 1321-1322.
(5) Stocking, E. M.; Williams, R. M. *Angew. Chemie. Int. Ed.* **2003**, *42* (27), 3078–3115.
(6) Auclair, K.; Sutherland, A.; Kennedy, J.; Witter, D. J.; Van den Heever, J. P.; Hutchinson, C. R.; Vederas, J. C. *J. Am. Chem. Soc.* **2000**, *122* (46), 11519–11520.
(7) Ose, T.; Watanabe, K.; Mie, T.; Honma, M.; Watanabe, H.; Yao, M.; Oikawa, H.; Tanaka, I. *Nature* **2003**, *422* (6928), 185–189.
(8) Ma, S. M.; Li, J. W.-H.; Choi, J. W.; Zhou, H.; Lee, K. K. M.; Moorthie, V. A; Xie, X.; Kealey, J. T.; Da Silva, N. A; Vederas, J. C.; Tang, Y. *Science* **2009**, *326* (5952), 589–592.
(9) Kim, R. R.; Illarionov, B.; Joshi, M.; Cushman, M.; Lee, C. Y.; Eisenreich, W.; Fischer, M.; Bacher, A. *J. Am. Chem. Soc.* **2010**, *132* (9), 2983–2990.
(10) Kim, H. J.; Ruszczycky, M. W.; Choi, S.; Liu, Y.; Liu, H. *Nature* **2011**, *473* (7345), 109–112.
(11) Fage, C. D.; Isiorho, E. A; Liu, Y.; Wagner, D. T.; Liu, H.; Keatinge-Clay, A. T. *Nat. Chem. Biol.* **2015**, *11* (4), 256–258.
(12) Hashimoto, T.; Hashimoto, J.; Teruya, K.; Hirano, T.; Shin-ya, K.; Ikeda, H.; Liu, H.; Nishiyama, M.; Kuzuyama, T. *J. Am. Chem. Soc.* **2015**, *137* (2), 572–575.
(13) Tian, Z.; Sun, P.; Yan, Y.; Wu, Z.; Zheng, Q.; Zhou, S.; Zhang, H.; Yu, F.; Jia, X.; Chen, D.; Mándi, A.; Kurtán, T.; Liu, W. *Nat. Chem. Biol.* **2015**, *11*, 259-265.
(14) Townsend, C. A. *Chembiochem* **2011**, *12* (15), 2267–2269.
(15) Kelly, W. L. *Org. Biomol. Chem.* **2008**, *6* (24), 4483–4493.
(16) Kim, H. J.; Ruszczycky, M. W.; Liu, H. W. *Curr. Opin. Chem. Biol.* **2012**, *16* (1-2), 124–131.
(17) Siegel, J. B.; Zanghellini, A.; Lovick, H. M.; Kiss, G.; Abigail, R.; Clair, J. L. S.; Gallaher, J. L.; Hilvert, D.; Gelb, M. H.; Stoddard, B. L.; Houk, K. N.; Michael, F. E.; Baker, D. *Science.* **2010**, *329* (5989), 309–313.
(18) Kim, S. P.; Leach, A. G.; Houk, K. N. *J. Org. Chem.* **2002**, *67* (3), 4250–4260.
(19) Eiben, C. B.; Siegel, J. B.; Bale, J. B.; Cooper, S.; Khatib, F.; Shen, B. W.; Players, F.; Stoddard, B. L.; Popovic, Z.; Baker, D. *Nat. Biotechnol.* **2012**, *30*, 190–192.
(20) Preiswerk, N.; Beck, T.; Schulz, J. D.; Milovník, P.; Mayer, C.; Siegel, J. B.; Baker, D.; Hilvert, D. *Proc. Natl. Acad. Sci. U. S. A.* **2014**, *111* (22), 8013–8018.
(21) Funel, J.-A.; Abele, S. *Angew. Chem., Int. Ed.* **2013**, *52* (14), 3822–3863.
(22) Riedlinger, J.; Reicke, A.; Zähner, H.; Krismer, B.; Bull, A. T.; Maldonado, L. A.; Ward, A. C.; Goodfellow, M.; Bister, B.; Bischoff, D.; Süssmuth, R. D.; Fiedler, H.-P. *J. Antibiot. (Tokyo).* **2004**, *57* (4), 271–279.
(23) Bister, B.; Bischoff, D.; Ströbele, M.; Riedlinger, J.; Reicke, A.; Wolter, F.; Bull, A. T.; Zähner, H.; Fiedler, H. P.;

Süssmuth, R. D. *Angew. Chemie. Int. Ed.* **2004**, *43* (19), 2574–2576.

(24) Gottardi, E. M.; Krawczyk, J. M.; Von Suchodoletz, H.; Schadt, S.; Mühlenweg, A.; Uguru, G. C.; Pelzer, S.; Fiedler, H. P.; Bibb, M. J.; Stach, J. E. M.; Süssmuth, R. D. *ChemBioChem* **2011**, *12* (9), 1401–1410.

(25) Vieweg, L.; Reichau, S.; Schobert, R.; Leadlay, P. F.; Süssmuth, R. D. *Nat. Prod. Rep.* **2014**, 1554–1584.

(26) Snider, B. B.; Zou, Y. *Org. Lett.* **2005**, *7* (22), 4939–4941.

(27) Neumann, P.; Brodhun, F.; Sauer, K.; Herrfurth, C.; Hamberg, M.; Brinkmann, J.; Scholz, J.; Dickmanns, A.; Feussner, I.; Ficner, R. *Plant Physiol.* **2012**, *160* (3), 1251–1266.

(28) Van Der Kamp, M. W.; Mulholland, A. J. *Biochemistry* **2013**, *52*, 2708–2728.

(29) Zheng, Q.; Guo, Y.; Yang, L.; Zhao, Z.; Wu, Z.; Zhang, H.; Liu, J.; Cheng, X.; Wu, J.; Yang, H.; Jiang, H.; Pan, L; Liu, W. *Cell Chem. Biol.* **2016**, *23*, 1-9.

TOC Artwork:

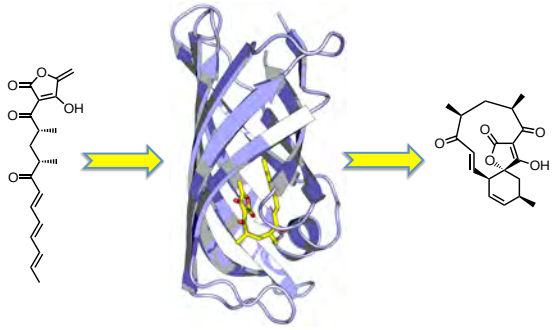

Diels-Alderase catalyzed [4+2] cycloaddition

Supporting information for:

The catalytic mechanism of a natural Diels-Alderase revealed in molecular detail

Matthew J. Byrne, Nicholas R. Lees, Li-Chen Han, Marc W. van der Kamp, Adrian J. Mulholland, James E.M. Stach, Christine L. Willis and Paul R. Race

This supplement includes:

Materials and Methods

1. Gene cloning

The gene encoding AbyU was amplified from *Verrucosispora maris* AB-18-032 genomic DNA by polymerase chain reaction (PCR) using the primers 5'-AAGTTCTGTTTCAGGGCCCGATGACTGAGCGACTGGAGACG-3' and 5'-ATGGTCTAGAAAGCTTTATCACGGATCCTGCTCGGCGAG-3', introducing appropriate overlap sequences (underlined) for insertion into the plasmid pOPINF,[1] pre-cut with *Kpn*I and *Hind*III. Ligations were carried out using the In-Fusion cloning kit (Clonetech) following the manufacturer's protocol. The resulting construct, *abyU*::pOPIN encodes an N-terminally hexa-histidine tagged variant of AbyU. The gene encoding the Leu73Met/Leu139Met AbyU double mutant (AbyU_DM) was amplified by PCR from a commercially sourced (MWG Eurofins™) plasmid containing a synthetic *abyU_DM* gene (fig. S3) using the primers 5'-AAGTTCTGTTTCAGGGCCCGATGACGGAACGCCTTGAAACC-3' (forward) and 5'-ATGGTCTAGAAAGCTTTATCATTCACCCATCAGAATGCG-3' (reverse), introducing appropriate overlap sequences (underlined) for insertion into the plasmid pOPINF, pre-cut with *Kpn*I and *Hind*III. Ligations were carried out using the In-Fusion cloning kit (Clonetech) following the manufacturer's protocol. The resulting construct, *abyU_DM*::pOPINF encodes an N-terminally hexa-histidine tagged variant of AbyU_DM. Leucine residues targeted for mutation to methionine residues in AbyU_DM, were selected based upon comparative sequence analysis of AbyU with known homologues of this protein. Methionine residues occupy positions equivalent to Leu73 and Leu139 in at least one other AbyU homologue. The sequences of all constructs were verified by DNA sequencing, following which each was transformed into *E. coli* B834(DE3) cells for protein expression.

2. Protein expression

The recombinant over-expression of AbyU and AbyU_DM was achieved using the same general procedure. Cultures of *E. coli* B834(DE3) cells harboring either *abyU*::pOPINF or, *abyU_DM*::pOPINF, were grown in 1 L Luria-Bertani (LB) medium, supplemented with 100 μg/mL carbenicillin, at 37 °C with shaking, until the optical density of the cultures at 600 nm had reached 0.6. Protein expression was induced by the addition of IPTG to a final concentration of 0.5 mM. Cultures were grown for an additional 16 hrs with shaking at 20 °C, following which cells were harvested by centrifugation, supernatant liquids removed, and the remaining cell pellets stored at −80 °C.

The recombinant over-expression of selenomethionine (SeMet) labeled AbyU_DM was achieved as follows. A culture of *E. coli* B834(DE3) cells harboring *abyU_DM*::pOPINF was grown in 10 mL of LB media, supplemented with 100 μg/mL carbenicillin, at 37 °C with shaking for 16 hrs. The cell culture was centrifuged, the supernatant liquid removed, and the remaining cell pellet resuspended in 1 mL of double-distilled water. This cell suspension was used to inoculate 1 L of M9 medium (preheated to 37 °C), supplemented with SelenoMethionine Medium Nutrient Mix (Molecular Dimensions), 50 mg of selenomethionine and 100 μg/mL carbenicillin. The culture was grown 37 °C with shaking, until the optical density at 600 nm had reached 0.6. At this point an additional 100 mg of selenomethionine was added and the cell suspension grown for an additional 30 minutes at 37 °C with shaking. The culture was induced by the addition of IPTG to a final concentration of 0.5 mM, following which it was grown for a further 16 hrs at 37 °C with shaking. Cells were harvested by centrifugation, the supernatant liquid removed, and the remaining cell pellet stored at −80 °C.

3. Protein purification

All recombinant proteins were purified using the same general strategy. Frozen cell pellets were thawed on ice and resuspended in 30 mL of His-Load buffer (20 mM Tris-HCl, 150 mM NaCl, 20 mM imidazole, pH 7.5) supplemented with an EDTA free protease inhibitor cocktail tablet (Roche). Cell suspensions were sonicated, and resulting cell lysates clarified by centrifugation, following which supernatant liquids were removed and applied to a 5 mL HisTrap column (GE life sciences) pre-charged with nickel. Each column was washed with 10 column volumes of His-Load buffer in order to remove any non-specifically bound proteins. Bound protein was eluted over 50 mL using a linear gradient of 0-50% His-Load to His-Elute buffer (20 mM Tris-HCl, 150 mM NaCl, 500 mM imidazole, pH 7.5), with fractionation (2 mL) throughout. For the purification of SeMet labeled AbyU_DM, His-Load and Elute buffers were supplemented with 2 mM TCEP. Fractions found to contain the target protein of interest, as established by monitoring the absorbance of the column eluent at 280 nm followed by SDS-PAGE analysis, were pooled and concentrated to 2 mL. For unlabeled recombinant AbyU and AbyU_DM, concentrated protein samples were applied to a 16/60 Superdex 75 column (GE life sciences), pre-equilibrated in 20 mM Tris-HCl, 150 mM NaCl, pH 7.5. For SeMet labeled recombinant AbyU_DM, concentrated protein samples were applied to a 16/60 Superdex 75 column (GE life sciences), pre-equilibrated in 20 mM Tris-HCl, 150 mM NaCl, 2 mM TCEP, pH 7.5. Fractions found to contain the target protein of interest, as determined by monitoring the absorbance of the column eluent at 280 nm followed by SDS-PAGE analysis, were pooled, concentrated to ~10 mg/mL, and flash frozen in liquid nitrogen for storage at −80 °C prior to use. SDS-PAGE and size exclusion chromatography analysis of all three recombinant proteins revealed that they were dimeric, homogeneous species in solution, of >95% purity (fig. S1).

4. AbyU enzyme activity assays

The ability of AbyU to accept the compounds **6** or **7** as substrates for [4+2] cycloaddition was assessed in 20 μL assay mixes comprising 280 μM AbyU, 10 mM **6** or **7**, 20 mM Tris-HCl, 150 mM NaCl, 10% methanol, pH 7.5. Assays were initiated by the addition of cold enzyme (4 °C) and incubated for 15 mins at 25 °C, following which they were quenched by the addition of 30 μL of ice-cold acetonitrile and centrifuged at 18000 rpm to remove precipitated protein. Control experiments were performed using the assay mixes and reaction conditions described above, but either excluding enzyme, or using heat denatured enzyme. For assays incorporating heat denatured enzyme a 100 μL 1 mg/ml solution of AbyU was heated at 100 °C for 10 minutes, following which appropriately sized aliquots of protein solution were removed and added to the assay mix. Assays to assess the ability of unlabeled and SeMet labeled AbyU_DM to catalyze [4+2] cycloaddition of **6** were performed using an identical approach to that outlined above.

Assay components were extracted in 2 × 1 mL of ethyl acetate and dried under a stream of nitrogen gas. Resulting residues were re-suspended in 100 μL of acetonitrile, of which 50 μL was subjected to LC-MS analysis. Chromatographic separations were performed using a Phenomenex LUNA column (5 μ, C_{18}, 100 Å, 4.6 × 250 mm), using a linear gradient of 10-90% acetonitrile/0.5% formic acid. Mass spectrometry was performed using a Waters ZQ Micromass spectrometer.

5. Elucidation of AbyU catalyzed and non-AbyU catalyzed reaction rates

Reaction rates for the conversion of **6** to **8** in the presence or absence of AbyU were determined spectrophotometrically by monitoring the rate of disappearance of **6** at 300 nm ($\varepsilon_{300\ nm}$ = 18400 $M^{-1}cm^{-1}$). All assays were performed in reaction buffer comprising 20 mM

Tris-HCl, 150 mM NaCl, pH 7.5, at 20 °C, using a 1 mm path length quartz cuvette, with a 1 mM stock solution of **6** dissolved in acetonitrile. For the calculation of the non-enzymatically catalysed conversion of **6** to **8**, 45 μM **6** was incubated in reaction buffer for 100 minutes and the change in absorbance monitored throughout. The resulting data were fitted to a single exponential of the form:

$$[A] = [A_0]e^{-kt}$$

Where $[A]$ is substrate concentration at time t, $[A_0]$ is substrate concentration at time 0, and k is the reaction rate.

To calculate the rate of the AbyU catalyzed conversion of **6** to **8**, **6** (0-200 μM) was incubated in reaction buffer with AbyU, at a final concentration of 1 nM. Initial rates were calculated by monitoring the change in absorbance for at least 1 minute, following which rates for the non-enzymatically catalysed conversion of **6** to **8** at each substrate concentration were subtracted. Background subtracted initial rates were plotted as a function of substrate concentration and fitted to a rectangular hyperbola of the form:

$$v_0 = \frac{k_{cat}[E][A]}{K_m + [A]}$$

Where v_0 is initial velocity, $[E]$ is enzyme concentration, $[A]$ is substrate concentration at time 0, k_{cat} is the enzyme catalyzed reaction rate and K_m is the Michaelis constant.

All reactions were repeated in triplicate. Data fitting was performed using GraphPad Prism.

6. Protein Crystallization

Conditions supporting the growth of crystals of unlabeled AbyU and SeMet labeled AbyU_DM were initially identified using the sitting drop vapor diffusion method at 18 °C, employing commercially available crystallization screens (Molecular Dimension Limited), mixing 0.2 μL of protein solution with 0.2 μL of reservoir solution. Diffraction quality crystals

of both proteins were grown using the hanging drop vapor diffusion method, employing reservoir solutions comprising 0.02 M magnesium chloride, 0.1 M HEPES pH 7.5, 18% w/v poly(acrylic acid) sodium salt MW 5100. Crystals took 3-5 days to grown to optimum size.

7. Diffraction data collection and structure determination

Crystals selected for diffraction data collection were mounted in appropriately sized litholoops (Molecular Dimensions Ltd), submerged in reservoir solution supplemented with 20% glycerol, and flash-cooled in liquid nitrogen prior to analysis. Diffraction data were collected at Diamond light source, UK, on beamlines I04-1 and I24. Diffraction data were processed with iMosflm,[2] and scaled and merged using Aimless [3], as implemented within the CCP4 suite of programs.[4] 5% of the data were set aside for the calculation of R_{free}. Identification of heavy atom sites and the resulting initial phase calculation was carried out using SHELX[5] employing data collected from crystals of SeMet labeled AbyU_DM. An initial model was built using the Autobuild pipeline in Phenix[6] and further extended using ARP/wARP[7] as implemented in the CCP4 suite of programs.[4] Iterative rounds of manual model building and refinement were carried out using COOT[8] and REFMAC.[9] The final AbyU_DM model comprises residues 10-140 of the native sequence, 99 water molecules, and 3 molecules of HEPES.

The structure of AbyU was determined by molecular replacement in PHASER,[10] using the AbyU_DM structure as a search model. The initial AbyU model was built using ARP/wARP,[7] followed by further iterative rounds of rebuilding and refinement with COOT[8] and REFMAC.[9] The final AbyU model comprises residues 6-141 of the native sequence, 76 water molecules, 5 molecules of glycerol, and 8 molecules of HEPES. Data collection, phasing and refinement

statistics for AbyU_DM and AbyU are provided in table S1. Protein structure figures have been prepared using PYMOL.[11]

8. Docking studies

Molecular docking of the natural substrate **4** and the bicyclic products **5** (the abyssomycin C precursor and its atropisomer) of AbyU was performed using the crystal structure complexed with HEPES. Chain A was used and the bound HEPES removed; selenomethionine was replaced with methionine. The substrate and product structures were initially built with GaussView and then optimized at the B97D/6-31+G(d,p) level. The substrate was optimized with C11-C12 in the *cis* conformation. AutoDockTools 1.5.4 was used to add Gasteiger charges, merge the non-polar hydrogens and define rotatable bonds for docking. In the substrate, the C11-C12 and C2-C3 bonds were defined as non-rotatable (to maintain the *cis* conformation and enforce positioning of the tetronate ring in line with the correct stereoisomer of the product, respectively) and all other formally single bonds were defined as rotatable. Subsequently, docking was performed with AutoDock Vina 1.1.2,[12] using a grid of 15 × 18 × 15 Å centered on the active site cavity, with side-chains of residues Tyr95, Phe113, Trp143 and Met145 (that line the cavity) defined with rotatable single bonds. The exhaustiveness was set to 25.

9. Molecular dynamics simulations

Explicit solvent molecular dynamics simulations were performed of the *apo*-enzyme and the complex with the bicyclic product **5** (the precursor of abyssomycin C). In all cases, chain A of the crystal structure of SeMet labeled AbyU_DM (complexed with HEPES) was used for the initial coordinates, with HEPES removed and selenomethionine replaced with methionine.

For the complexed structures (AbyU_DM with the bicyclic product), coordinates of the pose consistent with the 1st docking pose of the linear substrate were used, together with the side-chain positions of Tyr76, Phe95, Trp124 and Met126 obtained from docking. Hydrogens were added with the AmberTools program reduce; Asp43 was treated as protonated (predicted pK_a values by PropKa 3.1[13,14] were 9.7 and 11.1 for the *apo* and complexed structures, respectively) and His88 as doubly protonated (consistent with the hydrogen bonding network and a predicted pK_a value of 8.2). Missing heavy atoms were added using the AmberTools program tleap. Initial addition of water (at least 5 Å around the protein) was performed using the solvate program (http://www.mpibpc.mpg.de/grubmueller/solvate); 5 waters in the cavity in the *apo* simulations were kept and any waters in the cavity in the complexed structure were deleted. Subsequently, tleap was used to add additional waters to form a rectangular box (75 × 81 × 69 Å) and 3 sodium ions to neutralize the net charge.

MD simulations were performed with the Amber14 programs sander (for minimization) and pmemd.cuda (for MD on GPUs, using the default SPFP model)[15] and using the AMBER ff14SB force field for the protein,[16] the TIP3P water model and GAFF[17] for the products (parameters assigned with Antechamber). Particle-mesh Ewald summation was used in conjunction with periodic boundary conditions and a cut-off for direct-space non-bonded interactions of 8 Å. Partial charges of the products consistent with ff14SB were calculated using the PyRED server.[18] Prior to production simulation at 298 K and 1 atm, the following procedure was carried out: 1) optimize solvent and hydrogen positions (minimization for 300 steps followed by 50 ps langevin dynamics simulation in the NVT ensemble); 2) 300 steps of minimization and quick heating to 298 K (20 ps in NVT ensemble with 2 fs timestep, using langevin dynamics with SHAKE and initial random velocities assigned at 25K) with harmonic positional restraints on Cα atoms only (force constant: 5 kcal $mol^{-1}Å^{-2}$); 3) release of

positional restraints in 4 steps of 10 ps MD in the NPT ensemble (langevin dynamics with PME, SHAKE and timestep of 2 fs, a collision frequency of 1 and the Berendsen barostat with a pressure relaxation time of 1 ps); 4) 1 ns equilibration of temperature and pressure in the NPT ensemble (conditions as in previous step). Production simulation was then performed in the NVT ensemble using weak temperature control (MD with SHAKE and a 2 fs timestep, using the Berendsen thermostat with the time constant for coupling to the heat bath of 10 ps). Clustering analysis was performed with the AmberTools program cpptraj on the conformations sampled from 100 to 500 ns in the 4 apo simulations, based on the root-mean-square deviation of the heavy atoms in the 26-36 loop after alignment on the Cα atoms of the β-barrel. The Hierarchical Agglomerative approach was used with default settings and requesting 6 clusters. Root-mean-square fluctuations of Cα atoms were also calculated after alignment on the Cα atoms of the β-barrel.

10. QM/MM simulations

Approximate QM/MM umbrella sampling simulations at the SCC-DFTB/ff14SB level were performed starting from the 4 different poses of the AbyU product **5** obtained from docking (abyssomycin C, lacking the ether-bridge). Prior to QM/MM simulation, hydrogen atoms and a 20 Å sphere of water (TIP3P model) were added, centered on the spiro carbon of the product, and an initial MM structure optimization was performed. Thereafter, the product and the side chain of Trp124 were treated with the semi-empirical SCC-DFTB method[19] (a link atom was placed between Cα and Cβ in the Trp side chain), and the rest of the protein and water were treated with the ff14SB[16] and TIP3P force-fields, respectively. Atoms further than 20 Å from the central spiro carbon were held fixed to their starting positions. All QM/MM simulations were run using the Amber14 program sander, a 1 fs integration

timestep, a 10 Å cut-off for non-bonded interactions and in the NVT ensemble with temperature controlled with the Berendsen thermostat. After a short heating phase (10 ps with velocities assigned at 50 K, heating to 300 K with a 1 ps coupling constant to the heat bath), unbiased QM/MM MD simulations were run for each pose (at 300 K with a 4 ps coupling constant to the heat bath). Snapshots between 20 and 100 ps of QM/MM MD were used to start umbrella sampling. The *reaction coordinate* used to follow the Diels-Alder reaction was the distance between the center-of-mass of the dienophile carbons (C14, C15) and the center-of-mass of the diene carbons to which they bond (C13, C10). By using this reaction coordinate definition, no bias is applied as to which carbon-carbon bond is formed or broken first (or indeed whether or not the bonds are formed/broken synchronously). Umbrella sampling was performed using 26 windows from reaction coordinate values 1.3 Å to 3.8 Å (in steps of 0.1 Å). A restraint of 100 kcal $mol^{-1}Å^{-1}$ and 2 ps of simulation was used for each umbrella sampling window. Reaction coordinate values were recorded every 1 fs, and used for input to the Weighted Histogram Analysis Method (WHAM)[9] resulting in the potential of mean force (free energy) along the reaction coordinate. For each docking pose, at least 8 different snapshots from the unbiased QM/MM MD simulation were used to start QM/MM umbrella sampling along the reaction. Only for docking poses ranked 1 and 3, multiple consistent PMFs with a substrate minimum were obtained; for docking pose 2 no PMFs with a substrate minimum were obtained; for docking pose 4 only one reasonable PMF with a substrate minimum was obtained (and the SCC-DFTB SCF could not be converged in many simulation steps).

11. Gas phase DFT calculations

Transition states for the formation of the AbyU products **5** (the precursor of abyssomycin C and its atropisomer) in the gas phase were optimized at the M06-2X/6-31G(d,p) level,[20–22] using the QST3 method[23] in Gaussian09.[24] This functional, for which dispersion interactions were included in its parameterization, is suitable for modeling Diels-Alder reactions.[25] Transition states were confirmed using frequency calculations (indicating 1 imaginary frequency). Initial guesses for the 'reactant', transition state and 'product' geometries used as input for the QST3 calculations were obtained from relaxed scans at the B97D/6-31G(d,p) level, starting from the products. In order to generate a reasonable minimum energy path (without discontinuities; see Fig. S10B), scanning was performed first by increasing the C10-C15 distance up to ~2.4 Å, followed by scanning along the C13-C14 distance up to 2.6 Å whilst keeping C10-C15 fixed between 2.40-3.05 Å and finally scanning further along C13-C14 (up to 3.6 Å). All scans were performed in steps of 0.05 Å.

12. Electrostatic potential calculations

For figures that show an electrostatic potential projected on the molecular surface of protein X-ray crystal structures, the Poisson-Boltzmann electrostatic potential on the solvent accessible surface is shown, with potential values ranging from −15 kT/e (red) to 15 kT/e (blue). This was calculated with the APBS-plugin[26] in PyMOL, using a PQR file with AMBER force-field charges (ff99) after protonation state assignment by PropKa.[14]

13. Chemical synthesis

13.1 General experimental details

All reagents were sourced from commercial suppliers and were used without further purification unless stated otherwise. Where anhydrous conditions were necessary, standard Schlenk syringe-septa techniques were used with flame dried glassware under a positive pressure of nitrogen. Anhydrous THF, Et_2O, hexane and CH_2Cl_2 were dried by passing through a modified Grubbs system of alumina columns, manufactured by Anhydrous Engineering and stored over 3Å molecular sieves. All stated temperatures below ambient are the temperatures of the cooling baths, unless otherwise stated. Flash column chromatography was performed according to the procedures used by Still *et al.* using silica gel 60 (Fisher Scientific or Aldrich) and a suitable eluent. TLC was performed with aluminum backed silica TLC plates (Merck-Keiselgel 60 F254) with a suitable solvent system and was visualized using UV fluorescence (254 & 366 nm) and/or developed with potassium permanganate. Infra-red spectra were recorded on a Perkin Elmer Spectrum 100 FTIR with an ATR accessory and frequencies are reported in wavenumbers (cm^{-1}). ^{1}H and ^{13}C NMR spectra were recorded using Jeol ECP 400 MHz, Jeol ECS 400 MHz, Varian 400MR (400 MHz) and Varian VMR S500 MHz spectrometers at ambient temperature. Chemical shifts (δ) are quoted in parts per million (ppm) and coupling constants (J) are in Hertz (Hz). Tetramethylsilane or residual solvent peaks were used as the internal reference for proton and carbon chemical shifts. HRMS ESI were performed on either a Bruker Daltonics Apex 4, 7 Tesla FTICR or microTOF II. Samples were submitted in MeOH or CH_2Cl_2. Optical rotation ($[\alpha]_{TD}$) was measured on a Bellingham and Stanley Ltd. ADP220 polarimeter and is quoted in (° ml)(g dm)$^{-1}$

13.2 Organic synthesis of substrates and standards

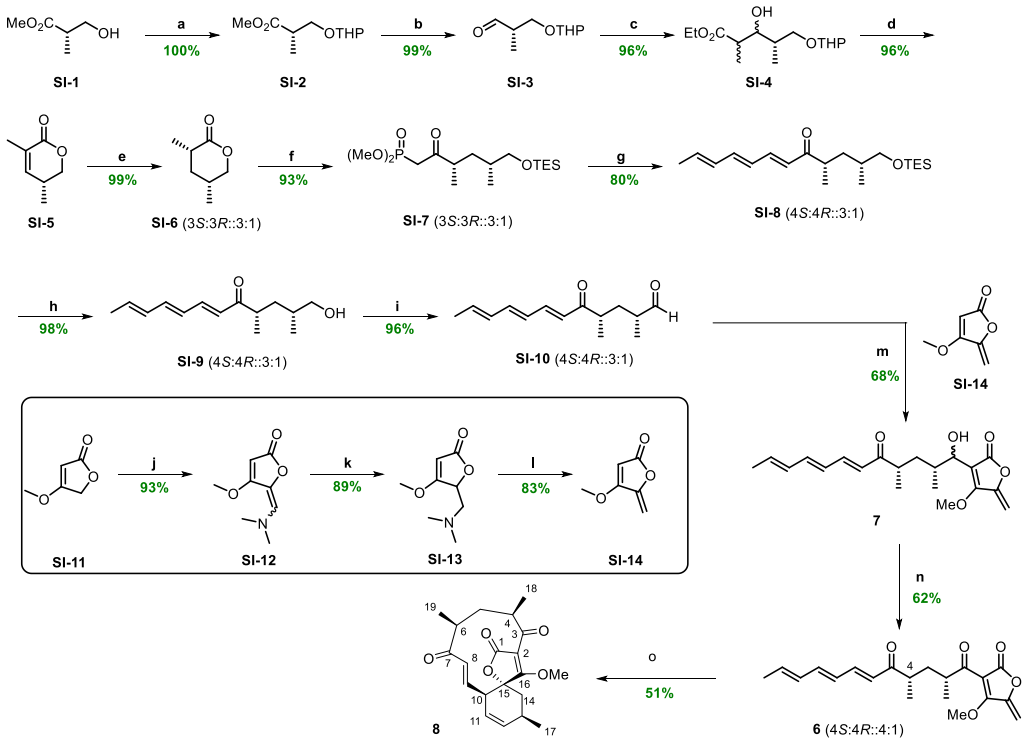

Reagents and condition: *a*) DHP (1.5 eq.), PPTS (0.15 eq.), CH_2Cl_2, rt, 16 h; *b*) DIBAL-H (1.05 eq.), CH_2Cl_2, –90 °C, 2 h; *c*) *i*-Pr_2NH (1.2 eq.), *n*-BuLi (1.2 eq.), ethyl propionate (1.2 eq.), THF, –15 to –78 °C, 1 h; *d*) (+)-CSA (1.2 eq.), C_6H_6, reflux, 14 h; *e*) H_2 (1 atm), Pd/C (10%), Et_2O, rt, 2 h; *f*) $(MeO)_2P(O)CH_3$ (1.1 eq.), *n*-BuLi (1.1 eq.), THF, –78 °C, then *n*-BuLi (1.1 eq.), TESCl (2.0 eq.), 14 h; *g*) *trans,trans*-2,4-hexadienal (1.2 eq.), $Ba(OH)_2$ (1.2 eq.), THF, H_2O, rt, 2 h; *h*) THF:AcOH:H_2O (12:3:2), rt, 2 h; *i*) BAIB (1.2 eq.), TEMPO (0.2 eq), CH_2Cl_2, rt, 2 h; *j*) dimethyl formamide dimethyl acetal, 110 °C, 8 h; *k*) 2 M HCl in Et_2O, $NaBH_3CN$ (1.01 eq.), MeOH, rt, 2 h; *l*) CH_3I (4 eq.), MeOH, 16 h, rt, then $NaHCO_{3(aq)}$, $CHCl_3$, rt, 2 h; *m*) *i*-Pr_2NH (1.2 eq.), *n*-BuLi (1.2 eq.), THF, 0 °C to –78 °C, 6 min; *n*) Dess-Martin periodinane (1.1 eq.), CH_2Cl_2, rt, 1 h; *o*) $CHCl_3$, hydroquinone, 70 °C, 2 days.

The synthetic approach to lactone **SI-5** was based upon that of Andrus *et al.*[27] Roche ester **SI-1** was THP protected followed by DIBAL-H reduction to aldehyde **SI-3** which underwent aldol addition with ethyl propionate to give aldol adduct **SI-4**. Treating aldol adduct with (+)-CSA in refluxing benzene deprotected the THP group and subsequent cyclization gave unsaturated lactone **SI-5**. Catalytic hydrogenation of **SI-5** gave the required *syn* lactone **SI-6** as the major diastereomer. Reaction of lactone **SI-6** with lithiated phosphonate ester gave **SI-7** which underwent a Horner-Wadsworth-Emmons olefination to give triene **SI-8**. TES deprotection and oxidation gave aldehyde **SI-10** (63% over 9 steps) which was coupled with the known tetronate **SI-14** (prepared in 3 steps and

69% overall yield from commercially available **SI-11** as previously described[28,29]) to give a mixture of epimeric alcohols **7.** Dess-Martin periodinane oxidation of **7** gave keto tetronate **6** (42% over 2 steps). Heating **6** in $CHCl_3$ in the presence of hydroquinone at 70 °C for 2 days[30] gave the Diels-Alder product, **8** which was used as a standard in the analysis of products from incubation studies with the enzyme AbyU.

(5*R*)-3,5-Dimethyl-5,6-dihydro-2*H*-pyran-2-one SI-5

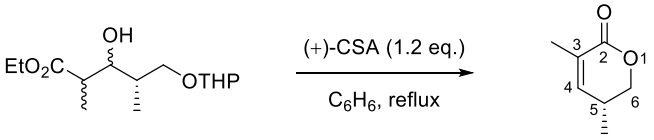

SI-4 **SI-5**

A mixture of isomers of known[27] hydroxy esters **SI-4** (4.33 g, 15.79 mmol) and (+)-CSA (4.65 g, 18.95 mmol) in benzene (160 mL) was refluxed for 16 h. The water generated was trapped by means of a Dean-Stark apparatus. The reaction mixture was allowed to cool to room temperature before the benzene was removed under reduced pressure and the residue was redissolved in CH_2Cl_2 (100 mL). The organic phase was washed with half saturated brine (200 mL) to remove the acid, dried over $MgSO_4$, concentrated then purified by vacuum distillation to give lactone **SI-5** (1.91 g, 96%) as a colorless liquid. **^{1}H NMR (400 MHz, $CDCl_3$): δ_H** 6.48 (1H, dd, *J* 3.0, 1.5, 4-H), 4.34 (1H, ddd, *J* 11.0, 5.0, 1.0, 6-H*H*), 3.99 (1H, dd, *J* 11.0, 8.5, 6-H*H*), 2.64 (1H, m, 5-H), 1.90 (3H, t, *J* 2.0, 3-CH_3), 1.09 (3H, d, *J* 8.5, 5-CH_3). **^{13}C NMR (100 MHz, $CDCl_3$): δ_C** 165.5 (C-2), 145.8 (C-4), 127.4 (C-3), 72.4 (C-6), 29.3 (C-5), 17.3 (3-CH_3) and 15.8 (5-CH_3). **FTIR** (neat) 1711 cm^{-1}. $[\alpha]_D^{20.7} = -32.6$ (*c* 0.12, $CDCl_3$), lit.[27] value = –34.7 (*c* 0.1, $CDCl_3$).

All data are in accordance with the literature.[27]

(3*S*,5*R*)-3,5-Dimethyltetrahydropyran-2-one SI-6

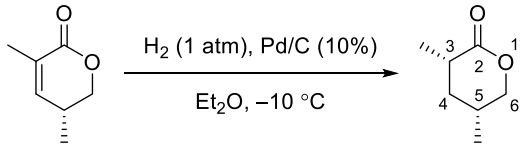

SI-5 **SI-6**

A mixture of lactone **SI-5** (2.62 g, 20.75 mmol) and Pd (10%)/Charcoal (2.21 g) was stirred in Et_2O (250 mL) at –10 °C (cryostat in *i*-PrOH) for 16 h under an atmosphere of H_2 (balloon). The reaction was monitored by TLC and was stopped when the spot no longer exhibited UV activity. The mixture was filtered through a plug of silica and filter paper to remove the Pd/C catalyst, the resulting solution was concentrated to give a near colorless oil (2.68 g, 99%). ^{1}H NMR showed the *cis*/*trans* ratio to be 3:1. **^{1}H NMR (400 MHz, $CDCl_3$): δ_H** (Major) 4.26 (1H, ddd, *J* 11.0, 4.5, 2.0, 6-*H*H), 3.76 (1H, dd, *J* 11.0, 9.0, 6-H*H*), 2.48 (1H, m, 3-H), 2.04 (2H, m, 4-H_2), 1.20 (3H, d, *J* 7.0, 3-CH_3), 1.15 (1H, m, 5-H), 0.93 (3H, d, *J* 6.5, 5-CH_3). **^{13}C NMR (100 MHz, $CDCl_3$): δ_C** 174.6 (C-2), 74.9 (C-6), 36.8, 35.3, 28.6, 17.4 (CH_3) and 16.9 (CH_3).

All data are in accordance with the literature.[27] After two recrystallizations from petrol (40/60) at 4 °C the ratio can be increased to 16:1 but with a poor recovery, 10% from 3:1 mixture.

Dimethyl (3*S*,5*R*)-3,5-dimethyl-2-oxo-6-(triethylsilyloxy)hexylphosphonate SI-7

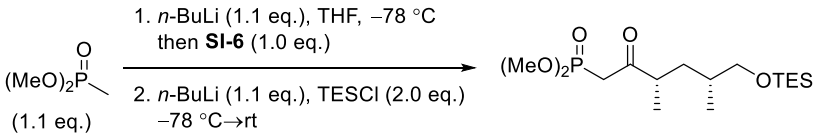

SI-7

To a solution of dimethyl methylphosphonate (1.17 ml, 10.82 mmol) in anhydrous THF (100 mL) at –78 °C was added *n*-BuLi (1.44 M, 7.51 mL, 10.82 mmol) and the reaction was stirred for 30 minutes under an atmosphere of nitrogen. A solution of lactone **SI-6** (1.26 g, 9.84 mmol) in anhydrous THF (5 mL) was added *via* syringe and the reaction was stirred for 1 h. *n*-BuLi (1.44 M, 7.51 mL, 10.82 mmol) was added dropwise and the reaction was stirred for 1 h. Et_3SiCl (3.3 mL, 19.68 mmol) was introduced and the reaction was slowly warmed to 25 °C overnight. The reaction was quenched with saturated NH_4Cl/H_2O/MeOH (3:6:1) and extracted with Et_2O (3 × 40 mL). The combined Et_2O extracts were washed with brine (50 mL), dried over $MgSO_4$, and concentrated to give crude **SI-7**. Flash chromatography on silica gel (2:1 to 1:2 *n*-hexane/Et_2O) gave **SI-7** (3.35 g, 93%) as a 3:1 mixture of diastereomers: **^{1}H NMR (400 MHz, $CDCl_3$): δ_H** (Major) 3.76 (6H, d, *J* 11.0, 2 × OCH_3), 3.46-3.37 (2H, m, 6-H_2), 3.18-3.03 (2H, m, 1-H_2), 2.88-2.79 (1H, m, 3-H), 1.79 (1H, ddd, *J* 13.5, 7.5, 6.0), 1.63-1.53 (1H, m), 1.09 (3H, d, *J* 7.0, CH_3), 1.05-0.99 (1H, m), 0.93 (9H, t, *J* 8.0, $Si(CH_2CH_3)_3$), 0.88 (3H, d, *J* 7.0, CH_3) and 0.56 (6H, q, *J* 8.0, $Si(CH_2CH_3)_3$). **^{13}C NMR (100 MHz, $CDCl_3$): δ_C** 205.8 (d, *J* 7, C-2), 67.8 (C-6), 52.0 (d, *J* 6.5, 2 × OCH_3), 52.08 (d, *J* C,P 6.5), 45.3 (d, *J* 2, C-3), 40.0 (d, *J* 131.0, C-1), 36.6, 33.6, 17.3, 16.9, 6.9 (3 × CH_3), 4.5 (3 × CH_2).

All data are in accordance with the literature.[30]

(2*R*,4*S*,6*E*,8*E*,10*E*)-2,4-Dimethyl-1-(triethylsilyloxy)dodeca-6,8,10-trien-5-one SI-8

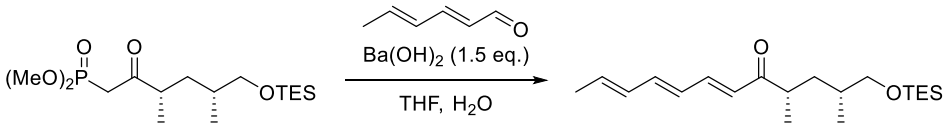

SI-7 **SI-8**

Phosphonate ester **SI-7** (1.01 g, 2.76 mmol) was dissolved in THF (reagent grade, 14.4 mL) and barium hydroxide (0.708 g, 4.13 mmol) was added. *trans*,*trans*-2,4-Hexadienal (0.364 ml, 3.31 mmol) in THF (47.5 mL) was added slowly to the stirring solution followed by water (9.5 mL) added dropwise and then stirred for 3 h. Brine (40 mL) was added, the layers separated and the aqueous layer extracted with EtOAc (3 × 40 mL), dried over $MgSO_4$ and concentrated *in vacuo*. The crude product was purified by flash chromatography eluting with 5-10% EtOAc in petroleum ether 40-60 °C to give silyl ether **SI-8** (0.742 g, 80%) as a near colorless oil in a 3:1 ratio of diastereomers: **^{1}H NMR (400 MHz, $CDCl_3$): δ_H** (Major) 7.23 (1H, dd, *J* 15.0, 11.0, 7-H), 6.57 (1H, dd, *J* 15.0, 11.0, 9-H), 6.26-6.13 (3H, m, 6-H, 8-H, 10-H), 6.00-5.95 (1H, dq, *J* 11.0, 7.0, 11-H), 3.44 (1H, distorted dd, *J* 9.5, 5.5), 3.38-3.33 (1H, m), 2.86 (1H, ddq, *J* 7.0), 1.83 (3H, d, *J* 7.0), 1.63-1.59 (1H, m), 1.16-1.07 (1H, m), 1.10 (3H, d, *J* 7.0), 0.94 (9H, t, *J* 8.0), 0.89 (3H, d, *J* 7.0), 0.58 (6H, q, *J* 8.0). **^{13}C NMR (100 MHz, $CDCl_3$): δ_C** 204.7 (C-5), 142.9 (C-7), 142.1 (C-9), 135.4 (C-11), 131.5 (C-10), 128.3 (C-8), 127.3 (C-6), 68.1 (C-1), 42.4 (C-4), 37.5 (C-3), 33.9 (C-2), 18.7 (C-12), 17.7 and 17.4 (2-CH_3 and 4-CH_3), 6.8 and 4.6 (Si(*C*H_2*C*H_3)$_3$).

All data are in accordance with the literature.[30]

(2*R*,4*S*,6*E*,8*E*,10*E*)-2,4-Dimethyl-1-hydroxy-dodeca-6,8,10-trien-5-one SI-9

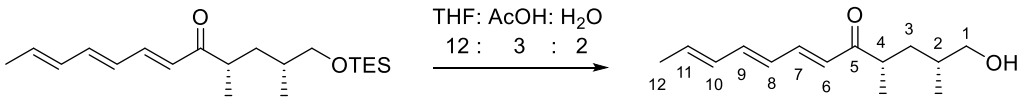

SI-8 **SI-9**

To a stirring solution of protected silyl ether **SI-8** (0.297 g, 0.87 mmol) in THF (12 mL) was added AcOH (3 mL) and H_2O (2 mL). The resulting yellow solution was stirred for 1 h and monitored by TLC. Upon full consumption of the starting material, the reaction was quenched by the slow addition of saturated $NaHCO_{3(aq)}$ until the evolution of CO_2 gas ceased. The aqueous layer was extracted with EtOAc (3 × 20 mL), combined organics were washed with brine (30 mL), dried over $MgSO_4$ and concentrated to give crude yellow oil which was purified by silica gel column chromatography eluting with 20% EtOAc in petroleum ether 40-60 °C to give alcohol **SI-9** as a yellow oil (0.193 g, 98%) in a 3:1 ratio of diastereomers: **^{1}H NMR (400 MHz, $CDCl_3$): δ_H** 7.26 (1H, dd, *J* 15.0, 11.0, 7-H), 6.58 (1H, dd, *J* 15.0, 10.5, 9-H), 6.26-6.14 (3H, m, 6-H, 8-H and 10-H), 5.96 (1H, m, 11-H), 3.48-3.38 (2H, m, 1-H_2), 2.84 (1H, m, 4-H), 1.96-1.86 (1H, m), 1.83 (3H, d, *J* 7.0, 12-H_3), 1.63 (1H, br. s., OH), 1.60-1.52 (1H, m), 1.22-1.14 (1H, m, 3-*H*H), 1.11 (3H, d, *J* 7.0, 4-CH_3), 0.93 (3H, d, *J* 7.0, 2-CH_3). **^{13}C NMR (100 MHz, $CDCl_3$): δ_C** 204.3 (C-5), 143.3 (C-7), 142.5 (C-9), 135.7 (C-11), 131.5 (C-10), 128.2 (C-8), 127.1 (C-6), 68.2 (C-1), 42.7 (C-4), 36.7 (C-3), 34.3 (C-2), 18.8 (CH_3), 18.5 (CH_3) and 17.4 (CH_3).

All data are in accordance with the literature.[30]

(2*R*,4*S*,6*E*,8*E*,10*E*)-2,4-Dimethyl-5-oxododeca-6,8,10-trienal SI-10

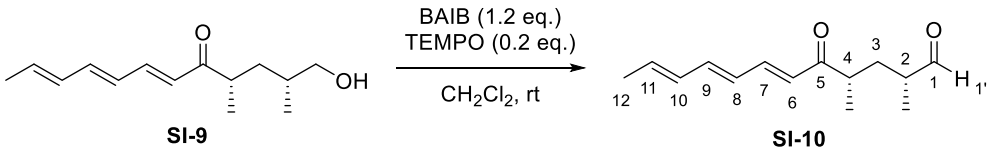

To a stirring solution of alcohol **SI-9** (0.187 g, 0.82 mmol) in anhydrous CH_2Cl_2 (5 mL) under an atmosphere of nitrogen was added (diacetoxyiodo)benzene (BAIB, 0.319 g, 0.99 mmol) and TEMPO (0.026 g, 0.17 mmol) and stirred at 23 °C for 3 h. TLC confirmed complete conversion of starting material, the reaction was quenched by the addition of saturated $Na_2S_2O_{3(aq)}$ (5 mL) and $NaHCO_{3(aq)}$ (1 mL) then stirred for a further 30 minutes. The layers were separated and the aqueous later was extracted with CH_2Cl_2 (3 × 15 mL). The combined organics were washed with brine (30 mL), dried over $MgSO_4$ and concentrated to give an orange oil. Silica gel chromatography was carried out eluting with 10-20% EtOAc in petroleum ether 40-60 °C to give aldehyde **SI-10** as a yellow oil (0.177 g, 96%) as a 3:1 ratio of diastereomers. **^{1}H NMR (400 MHz, $CDCl_3$): δ_H** 9.60 (1H, d, *J* 2.0, CHO), 7.27 (1H, m, 7-H), 6.59 (1H, ddd, *J* 14.5, 10.5, 4.0, 9-H), 6.27-6.09 (3H, m, 6-H, 8-H and 10-H), 5.97 (1H, dq, *J* 14.5, 7.0, 11-H), 2.85 (1H, sextet, *J* 7.0, 4-H), 2.36 (1H, m, 2-H), 2.19 (1H, dt, *J* 14.5, 7.5, 3-*H*H), 1.83 (3H, d, *J* 7.0, 12-H_3), 1.35-1.24 (1H, m, 3-H*H*), 1.12 (3H, d, *J* 7.0, 4-CH_3), 1.09 (3H, d, *J* 7.0, 2-CH_3). **^{13}C NMR (100 MHz, $CDCl_3$): δ_C** 204.6 (C-1), 203.0 (C-5), 143.7 (C-7), 142.7 (C-9), 135.9 (C-11), 131.5 (C-10), 128.1 (C-8), 127.0 (C-6), 44.4 (C-2), 41.8 (C-4), 33.7 (C-3), 18.8 (C-12), 17.7 (CH_3) and 13.9 (CH_3).

All data are in accordance with the literature.[30]

(2*R*,4*S*,6*E*,8*E*,10*E*)-1-Hydroxy-1-(5'-methoxy-4'-methylene-2'-oxo-2',4'-dihydrofuran-1'-yl)-2,4-dimethyldodeca-6,8,10-triene-5-one 7

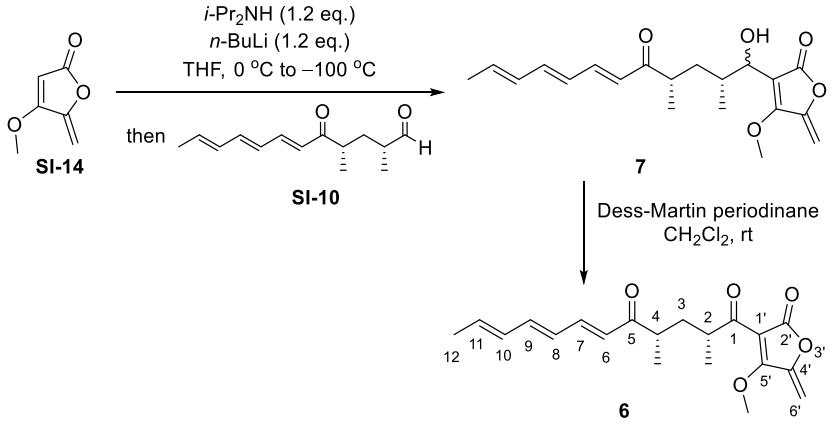

n-BuLi (1.41 M, 0.494 mL, 0.696 mmol) was added dropwise to a stirred solution of *i*-Pr_2NH (0.098 mL, 0.696 mmol) in anhydrous THF (5.4 mL) under an atmosphere of nitrogen at 0 °C for 30 minutes. The LDA solution was cooled to −100 °C, a solution of lactone **SI-14** (0.073 g, 0.58 mmol) in anhydrous THF (2.7 mL) was added *via* cannula, and the solution was stirred for 6 minutes at −100 °C as a pale yellow solution. A solution of aldehyde **SI-10** (0.128 g, 0.58 mmol) in anhydrous THF (3.4 mL) was added slowly *via* cannula. The resulting solution was stirred at −100 °C for 1 h to form an orange solution, quenched with saturated $NH_4Cl_{(aq)}$ (20 mL), and slowly warmed to 25 °C. The layers were separated, and the aqueous layer was extracted with EtOAc (3 × 40 mL). The combined organic layers were washed with brine (40 mL), dried over $MgSO_4$, and concentrated. Flash chromatography eluting with 10-20% EtOAc in petroleum ether 40-60 °C gave **7** as a near colorless oil (0.138 g 68 %) as a mixture of epimers which was used directly in the next step.

Dess-Martin periodinane (15% wt., 0.45 mL, 0.159 mmol) was added to a solution of tetronate **7** (0.050 g, 0.145 mmol) in CH_2Cl_2 (6 mL) and stirred at room temperature for 1 h. TLC confirmed complete conversion of starting material to a less polar product. The reaction was quenched by the addition of saturated $Na_2S_2O_{3(aq)}$ (10 mL) and $NaHCO_{3(aq)}$ (2 mL) stirred for a further 30 minutes. The layers were separated and the aqueous later was extracted with CH_2Cl_2 (3 x 20 mL). The combined organics were washed with brine (15 mL), dried over $MgSO_4$ and concentrated. Standard silica gel chromatography was carried out eluting with 10-20% EtOAc in petroleum ether 40-60 °C to give **6** as a pale yellow oil (0.031 g, 62%) as a 4:1 mixture of diastereomers. **^{1}H NMR (500 MHz, $CDCl_3$): δ_H** (Major) 7.24 (1H, dd, *J* 15.0, 11.0, 7-H), 6.59 (1H, dd, *J* 15.0, 11.0, 9-H), 6.29-6.08 (3H, m, 6-H, 8-H and 10-H), 5.96 (1H, m, 11-H), 5.25 (1H, d, *J* 3.0, 6'-*H*H), 5.20 (1H, d, *J* 3.0, 6'-H*H*), 4.10 (3H, s, OCH_3), 3.64 (1H, m, 2-H), 2.80 (1H, m, 4-H), 2.22 (1H, m, 3-*H*H), 1.82 (3H, d, *J* 7.0, 12-H_3), 1.32 (1H, m, 3-H*H*), 1.14 (3H, d, *J* 6.5, 2-CH_3) and 1.12 (3H, d, *J* 6.5, 4-CH_3). **^{13}C NMR (125 MHz, $CDCl_3$): δ_C** 203.2 (C-5), 200.5 (C-1), 168.5 (C-5'), 166.2 (C-2'), 148.8 (C-4'), 143.2 (C-7), 142.1 (C-9), 135.3 (C-11), 131.4 (C-10), 128.2 (C-8), 127.2 (C-6), 104.6 (C-1'), 95.7 (C-6'), 62.7 (OCH_3), 42.2 (C-2), 42.0 (C-4), 35.6 (C-3), 18.6 (C-12), 17.8 (2-CH_3), 16.9 (4-CH_3).

All data are in accordance with the literature.[30]

Diels-Alder adduct 8

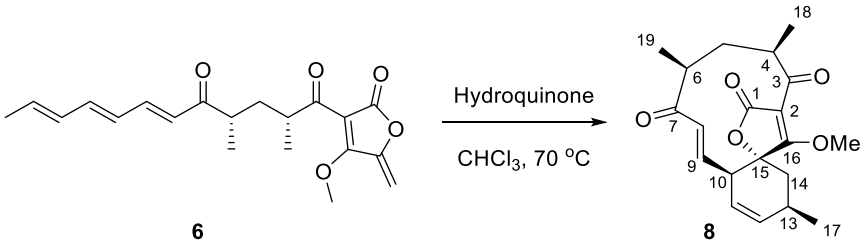

6 **8**

Tetronate **6** (57 mg, 0.167 mmol) and hydroquinone (1 mg) was dissolved in $CHCl_3$ (5 mL) and heated in a sealed tube at 75 °C for 2 days. The reaction mixture was cooled to room temperature and concentrated to give 44 mg of crude compound. A portion of the crude was purified (20 mg) by silica gel chromatography (10-20% EtOAc in petroleum ether 40-60 °C) to give Diels-Alder adduct **8** (29 mg, 51%) as a 4:1 mixture of diastereomers. **^{1}H NMR (500 MHz, $CDCl_3$): δ_H** (Major) 6.46 (1H, dd, *J* 16.5, 7.0, 9-H), 6.24 (1H, d, *J* 16.5, 8-H), 5.85 (1H, app. dt, *J* 10.0, 3.0, 12-H), 5.67 (1H, app. dt, *J* 10.0, 3.0, 11-H), 3.90 (3H, s, OMe), 3.44 (1H, m, 10-H), 3.11 (1H, m, 4-H), 2.94 (1H, sextet, *J* 6.5, 6-H), 2.63 (1H, m, 13-H), 2.39 (1H, dd, *J* 14.5, 8.0, 14-H*H*), 1.86 (1H, ddd, *J* 15.0, 6.0, 4.0, 5-*H*H), 1.81 (1H, dd, *J* 14.5, 4.5, 14-*H*H), 1.18 (1H, overlapping m, 5-H*H*), 1.20 (3H, d, *J* 7.0, 19-H_3), 1.18 (3H, d, *J* 6.5, 18-H_3), 1.14 (3H, d, *J* 7.5, 17-H_3). **^{13}C NMR (125 MHz, $CDCl_3$): δ_C** 204.3 (C-7), 200.6 (C-3), 178.2 (C-16), 169.9 (C-1), 141.5 (C-9), 136.7 (C-12), 131.6 (C-8), 121.8 (C-11), 106.9 (C-2), 86.0 (C-15), 61.7 (O*C*H_3), 46.63 (C-4), 46.57 (C-6), 44.6 (C-10), 38.9 (C-5), 36.6 (C-14), 29.3 (C-13), 21.1 (C-17), 17.0 (C-19) and 16.6 (C-18).

All data are in accordance with the literature.[30]

Diels-Alder adduct 8 from incubation of alcohols 7 with AbyU followed by purification then oxidation

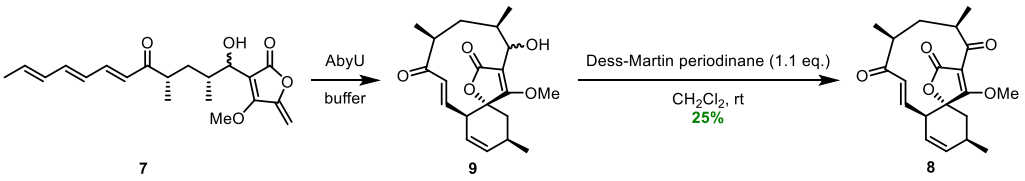

7 9 8

Alcohol **9** (0.8 mg, 2.513 µmol) obtained from purification by prep-TLC (100% CH_2Cl_2) of the product from incubation of alcohols **7** with AbyU was dissolved in anhydrous CH_2Cl_2 (0.103 mL) and was cooled to 0 °C under an atmosphere of nitrogen. Dess-Martin periodinane (15% wt., 8 µL) was added, and then the reaction was stirred at room temperature for 1 h. Saturated $NaHCO_{3(aq)}$ (2 mL) was added and the aqueous phase was extracted with Et_2O (3 × 5 mL). The combined organic layers were dried over $MgSO_4$, filtered and concentrated *in vacuo*. The crude product was purified by prep-TLC (50-100% CH_2Cl_2 in petroleum ether 40-60 °C) giving ketone **8** (0.2 mg, 25%) as a colorless oil. The ^{1}H-NMR spectrum correlates with synthetic **8** and the literature.[30]

12.3 NMR SPECTRA

(5*R*)-3,5-Dimethyl-5,6-dihydro-2*H*-pyran-2-one SI-5

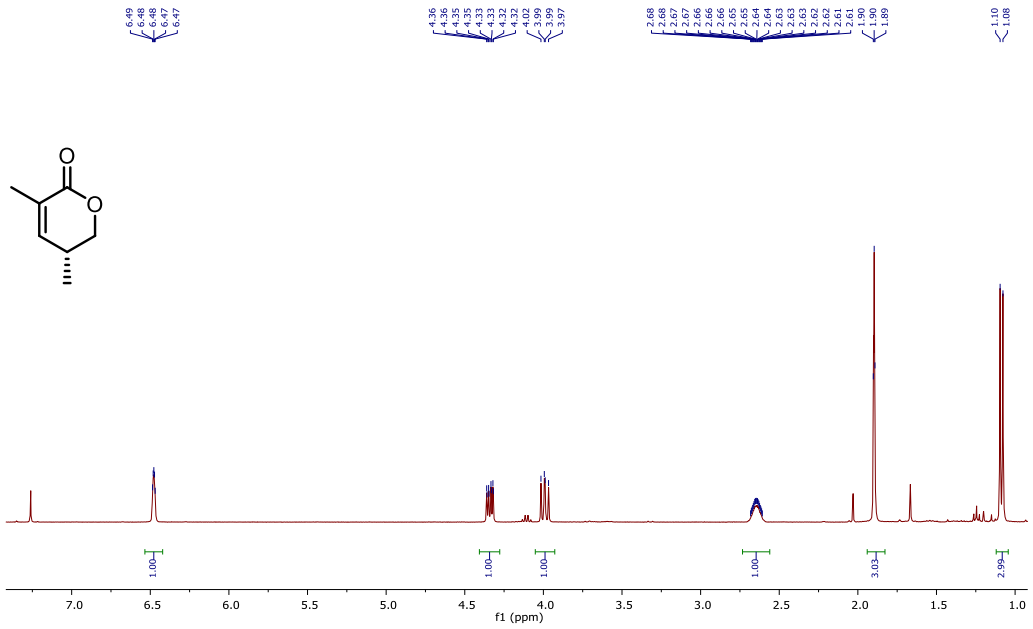

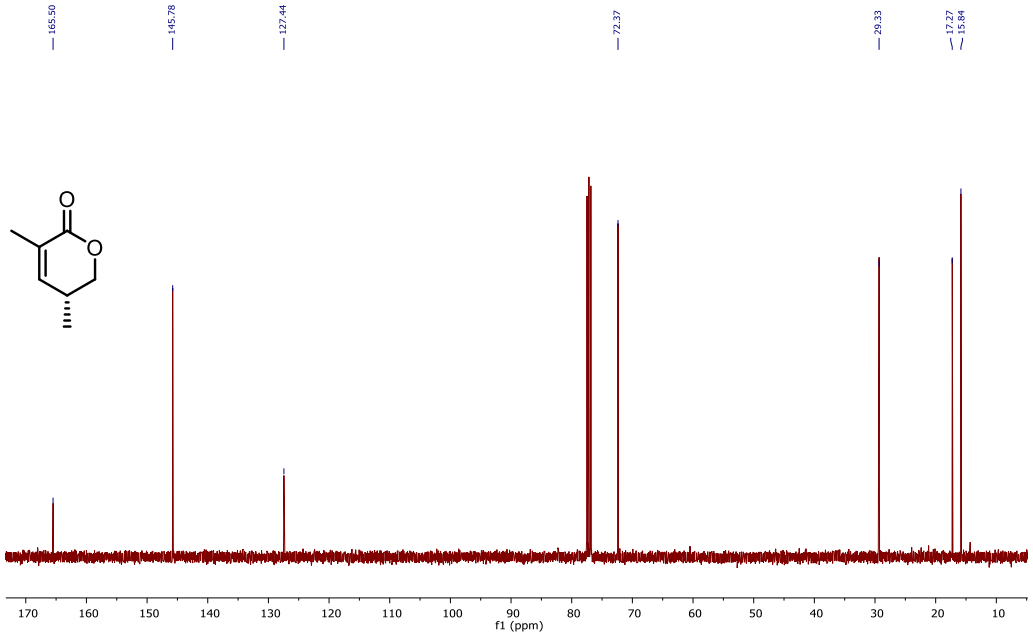

(3*S*,5*R*)-3,5-Dimethyltetrahydropyran-2-one SI-6

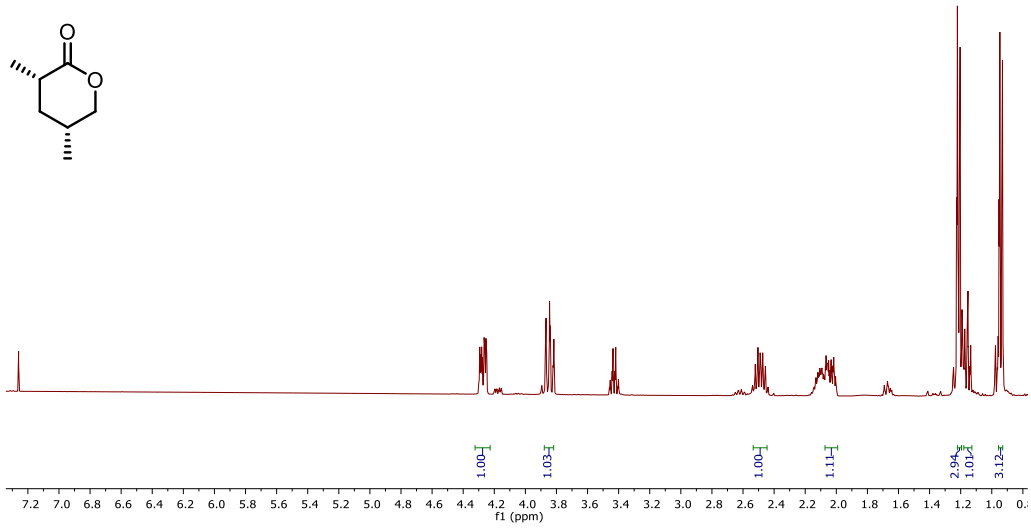

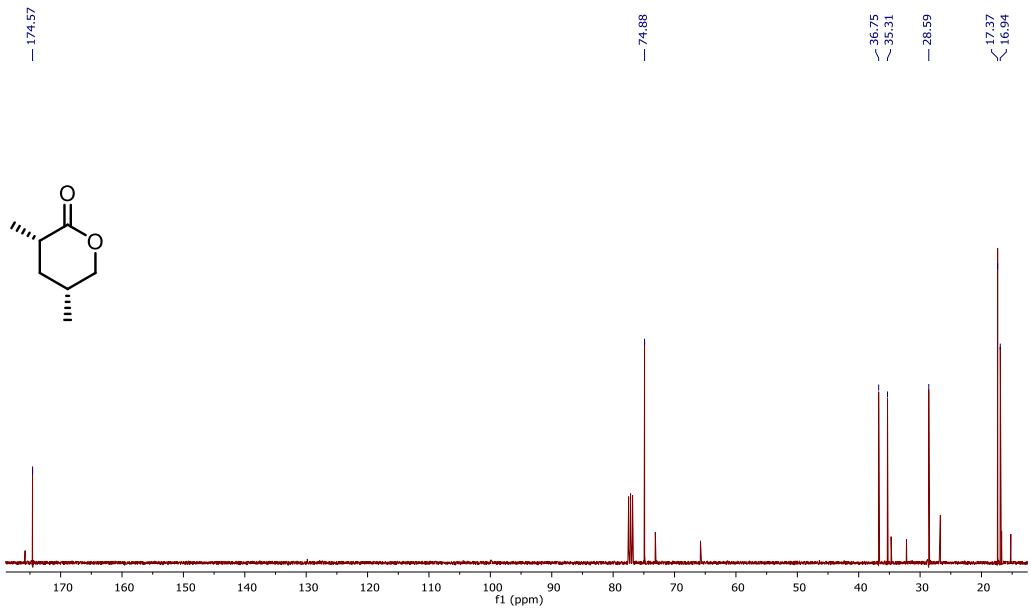

Dimethyl (3*S*,5*R*)-3,5-dimethyl-2-oxo-6-(triethylsilyloxy)hexylphosphonate SI-7

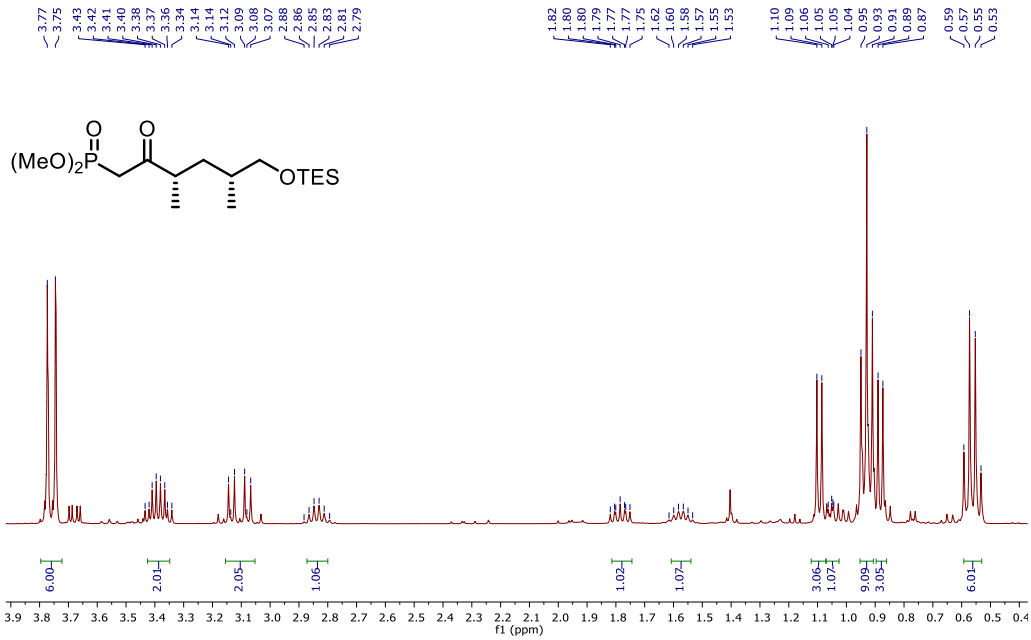

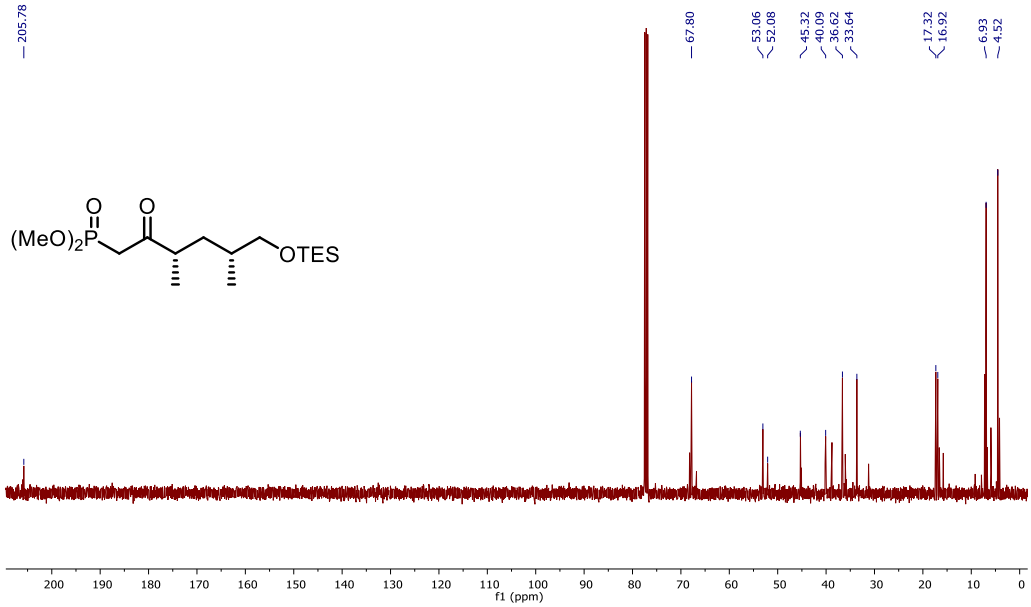

(2*R*,4*S*,6*E*,8*E*,10*E*)-2,4-Dimethyl-1-(triethylsilyloxy)dodeca-6,8,10-triene-5-one SI-8

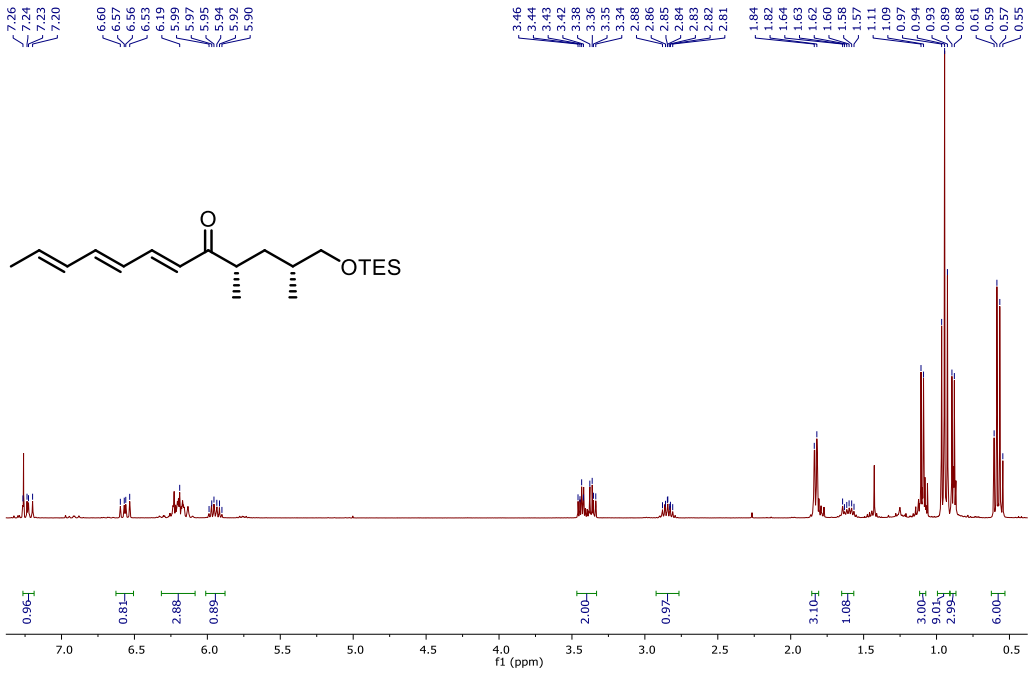

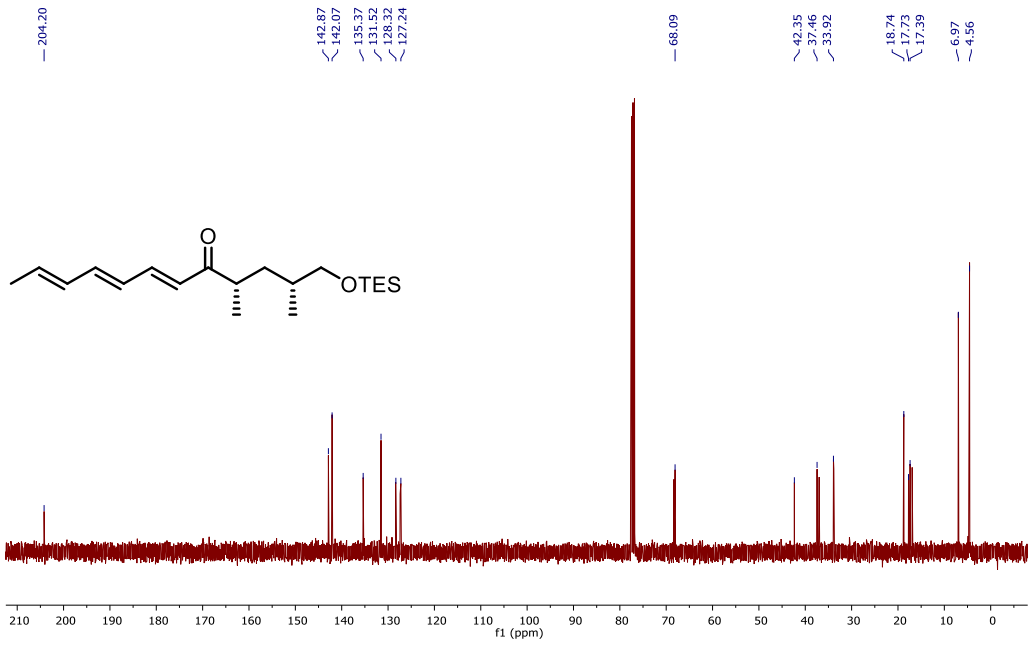

(2*R*,4*S*,6*E*,8*E*,10*E*)-2,4-Dimethyl-1-(triethylsilyloxy)dodeca-6,8,10-triene-5-one SI-8

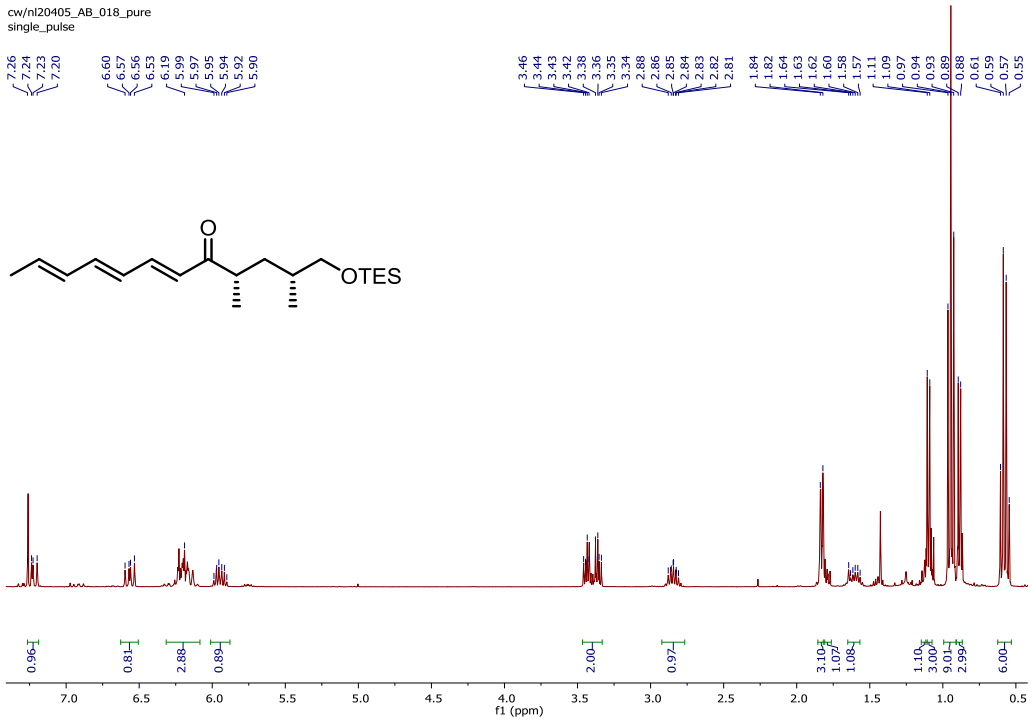

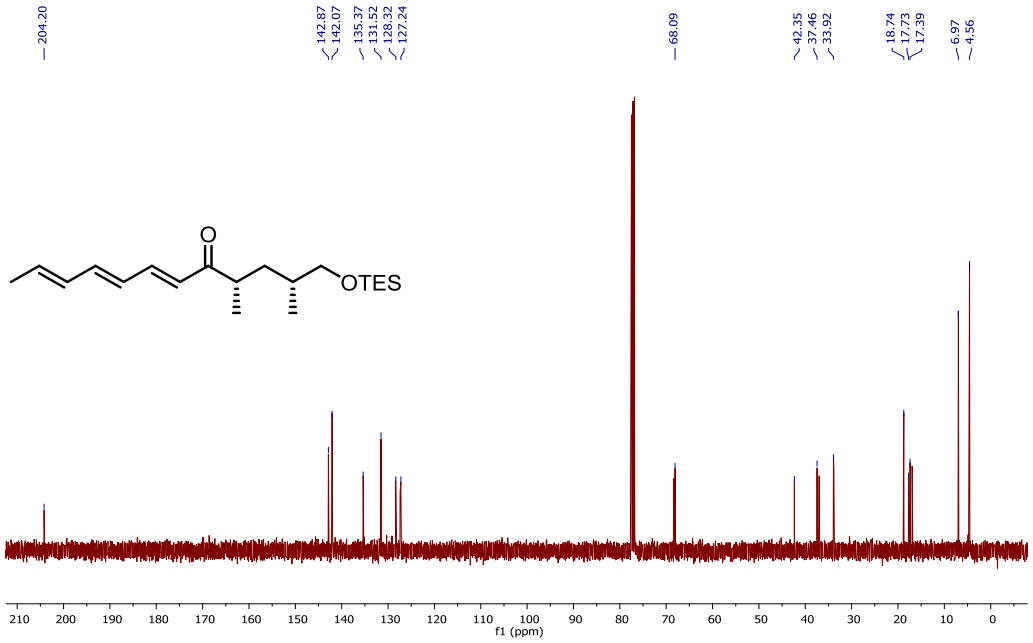

(2*R*,4*S*,6*E*,8*E*,10*E*)-2,4-Dimethyl-1-hydroxy-dodeca-6,8,10-trien-5-one SI-9

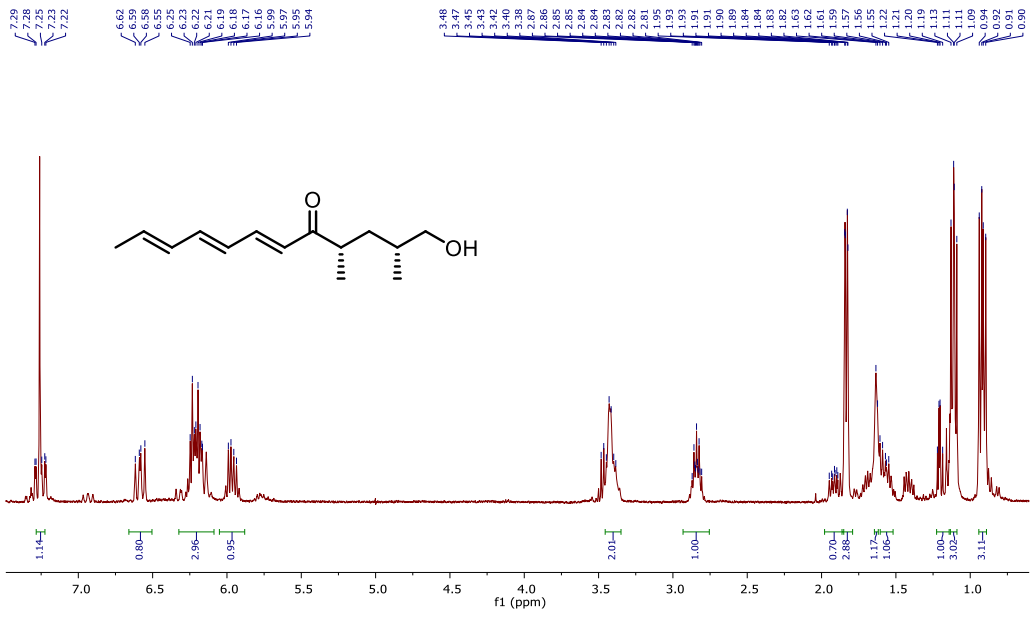

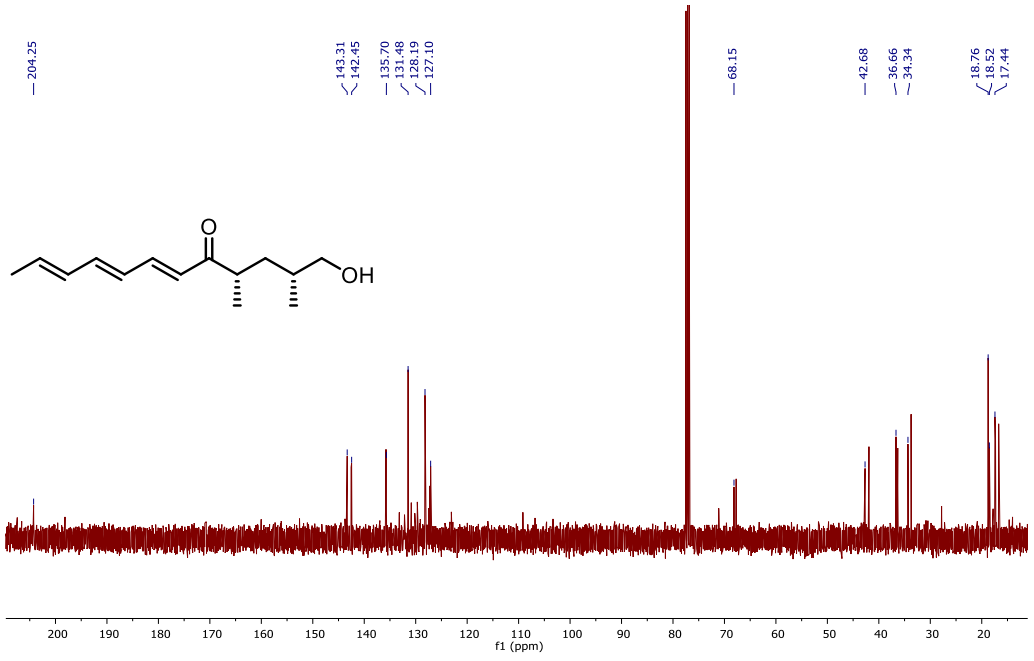

(2*R*,4*S*,6*E*,8*E*,10*E*)-2,4-Dimethyl-5-oxododeca-6,8,10-trienal SI-10

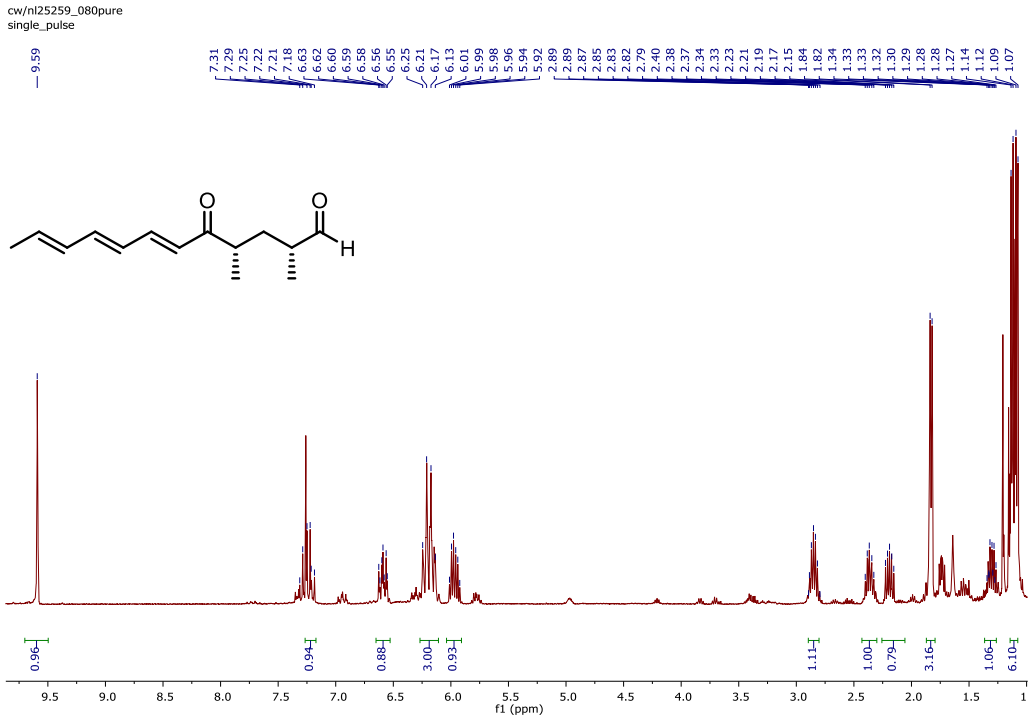

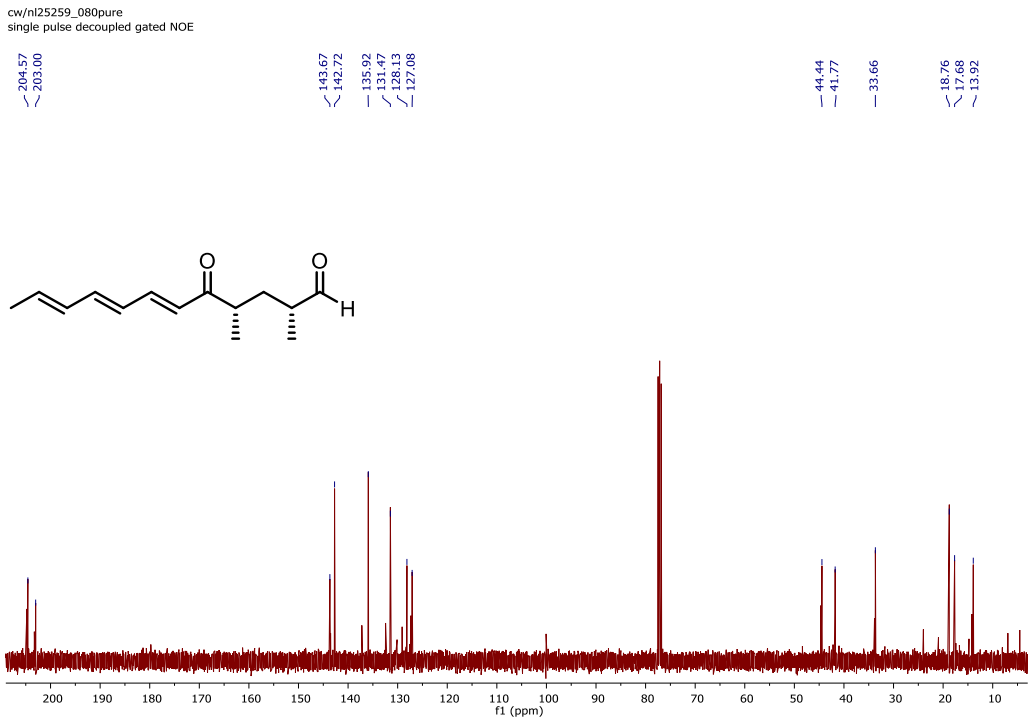

4-Methoxy-5-methylenefuran-2(5*H*)-one SI-14

nl126190_NL_AB_200_pure_PROTON_01

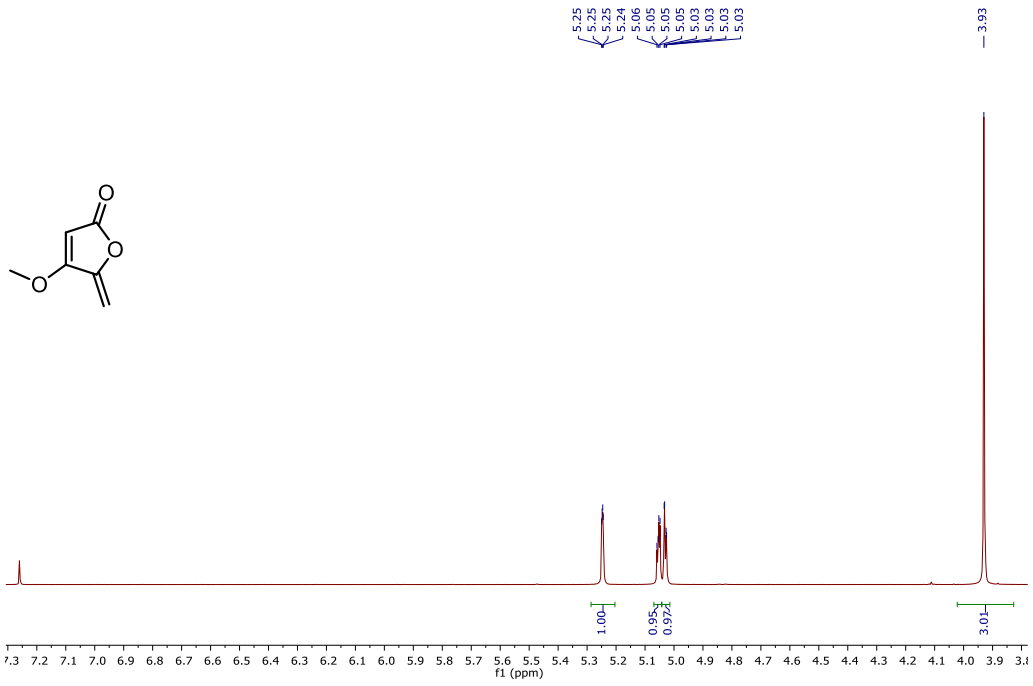

cw/nl15937_AB_200p
single pulse decoupled gated NOE

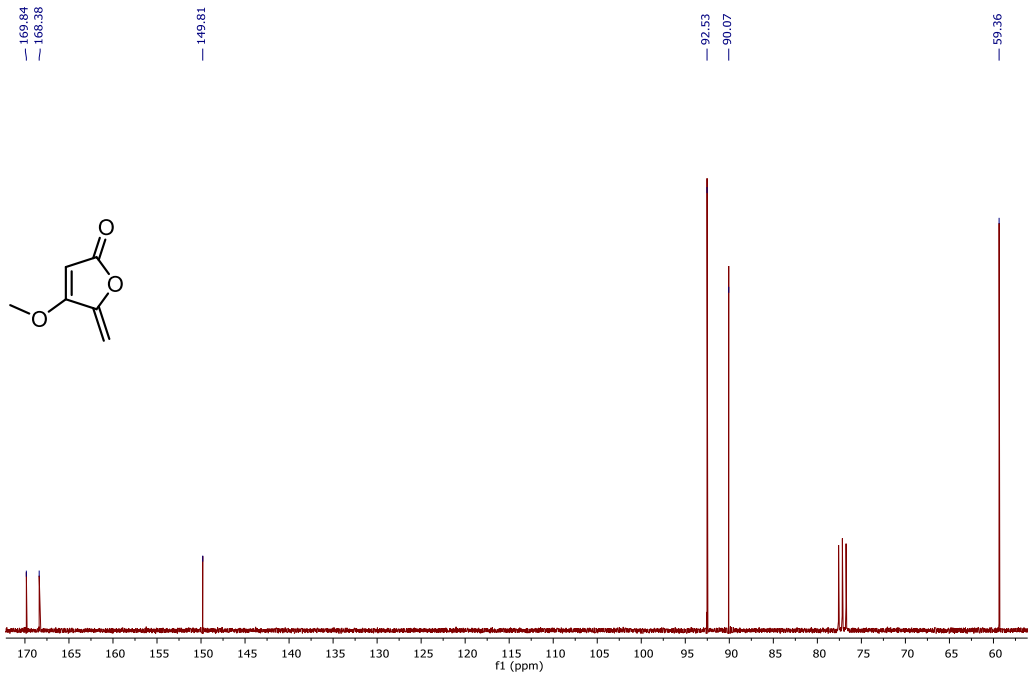

(2*R*,4*S*,6*E*,8*E*,10*E*)-1-(5'-methoxy-4'-methylene-2'-oxo-2',4'-dihydrofuran-1'-yl)-2,4-dimethyldodeca-6,8,10-triene-1,5-dione 6

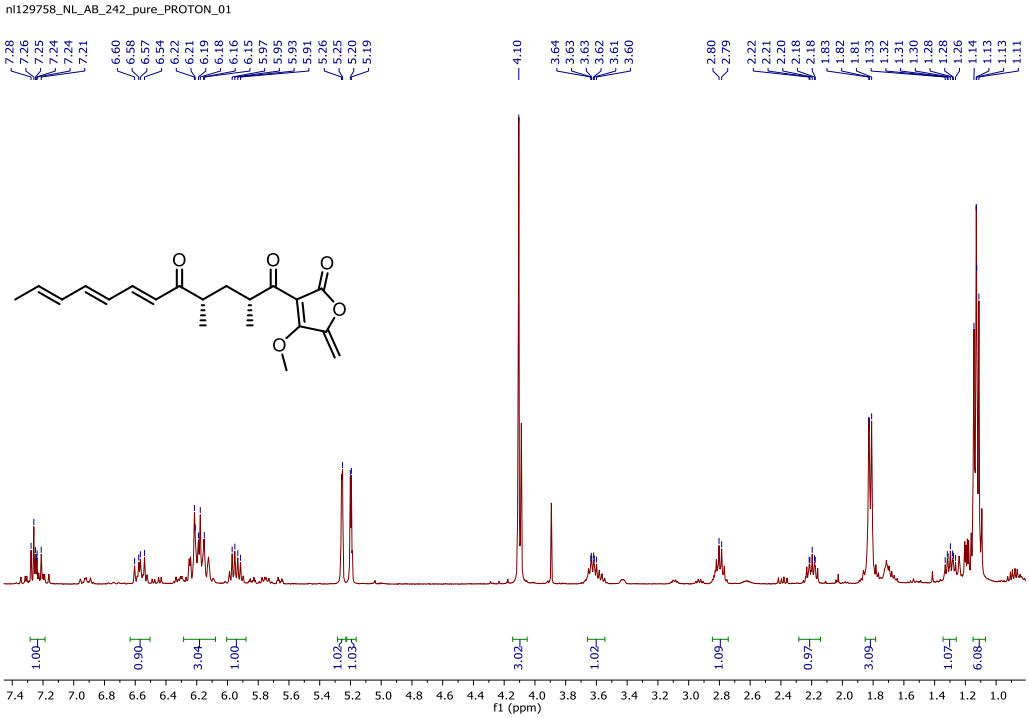

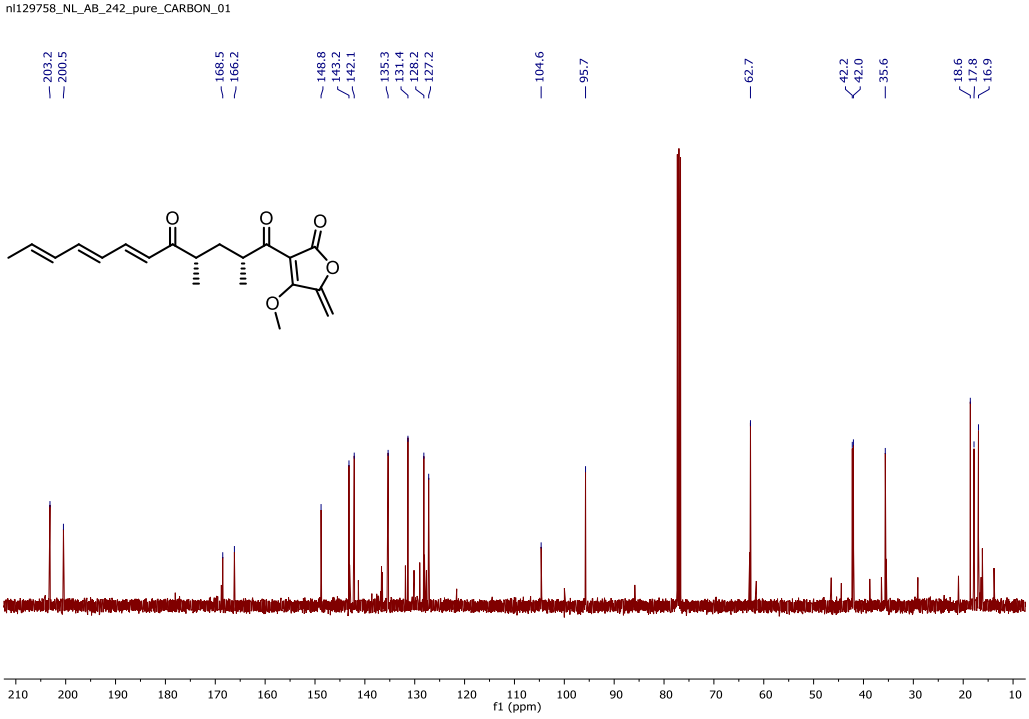

Diels-Alder adduct 8

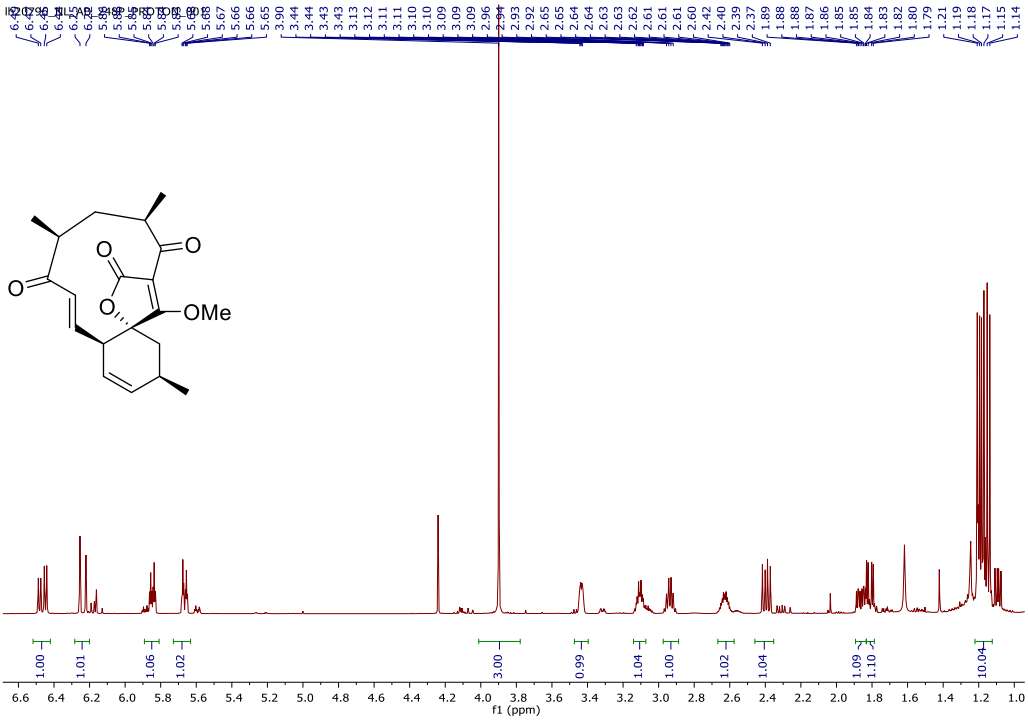

lh20796_NL_AB_248P_CARBON_001

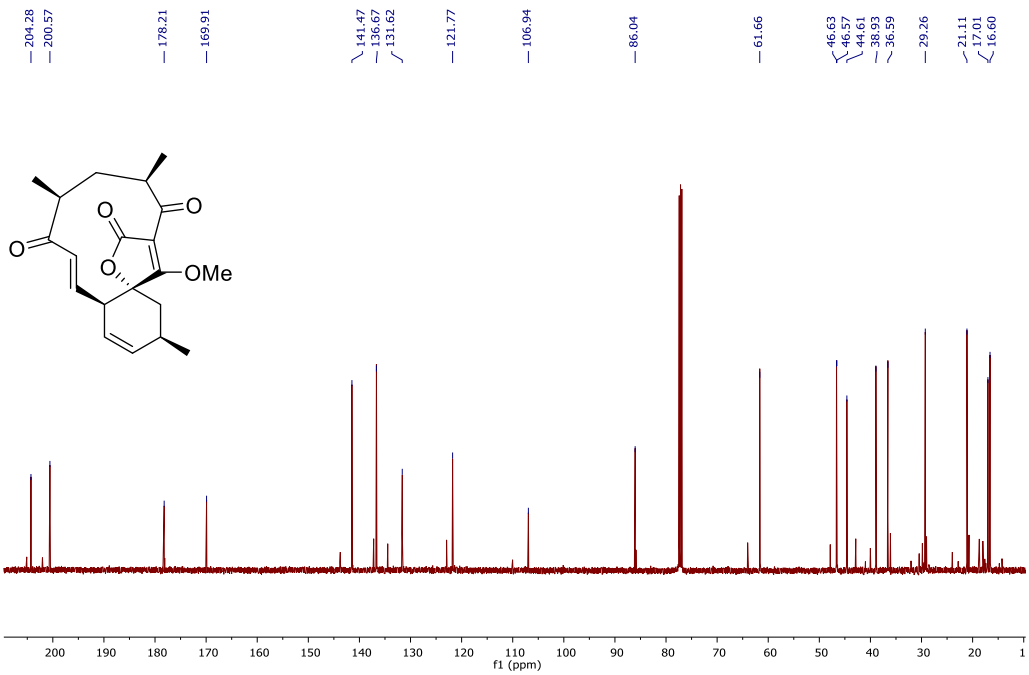

Comparison on ^{1}H NMR of synthetic Diels-Alder adduct 8 (top) with Diels-Alder adduct 8 from incubation of alcohols 7 with AbyU followed by purification then oxidation (bottom)

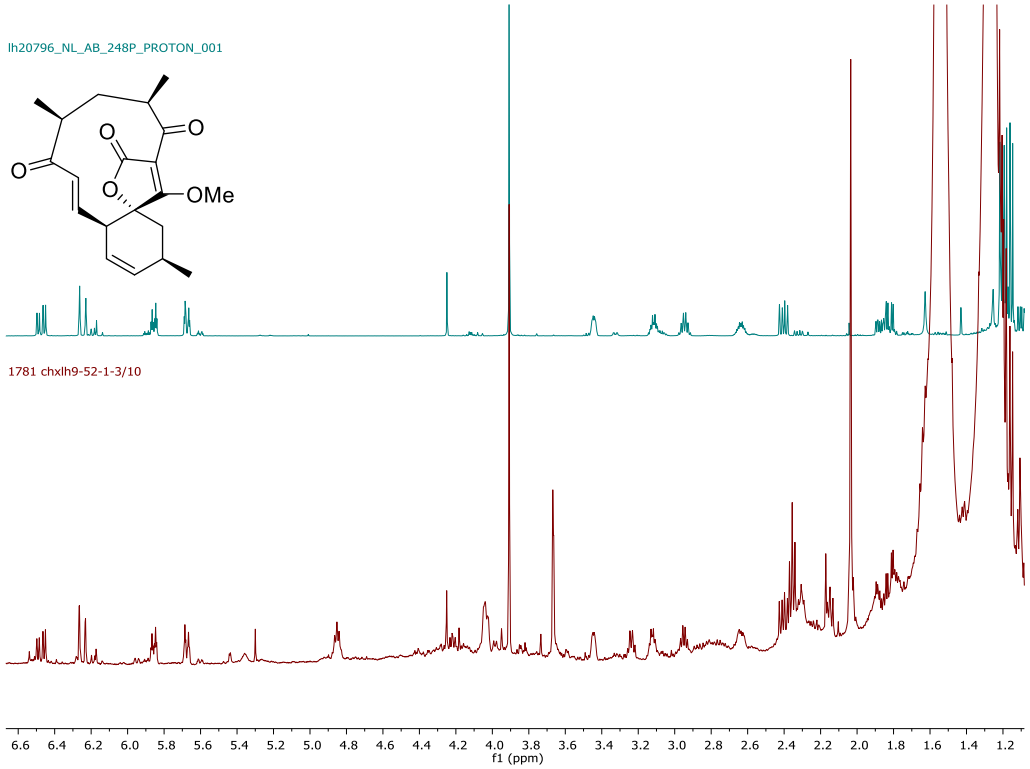

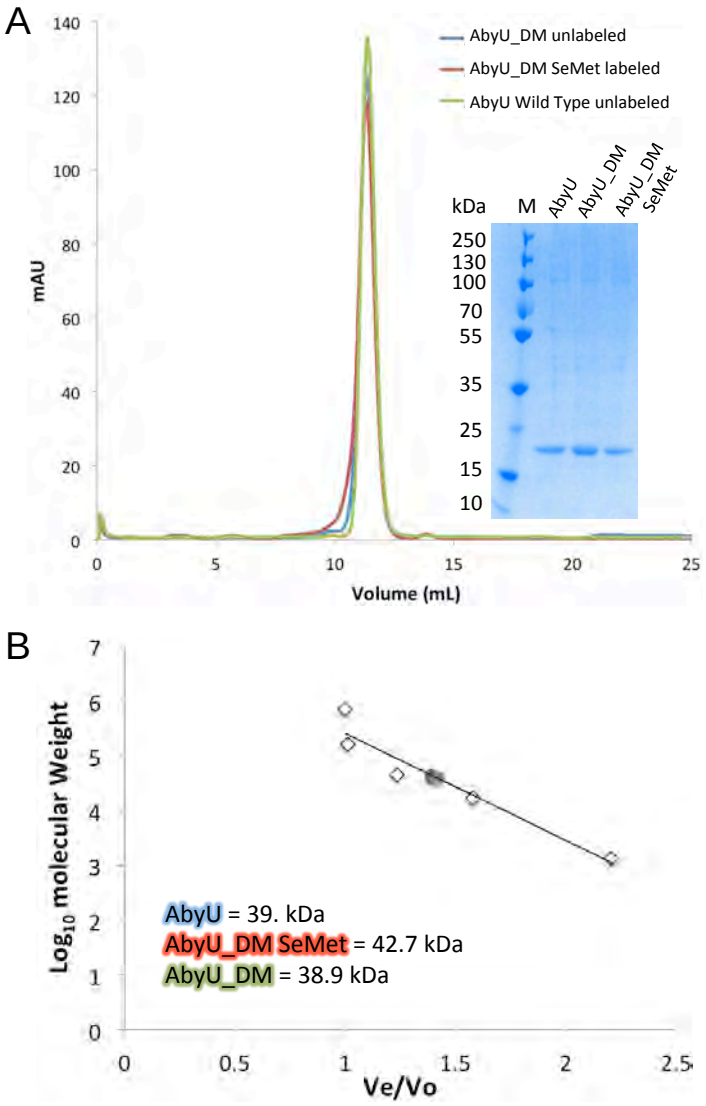

Fig. S1. Size exclusion chromatography and SDS-PAGE analysis of purified recombinant AbyU, AbyU_DM and SeMet labeled AbyU_DM. A, Chromatogram showing the elution profiles of AbyU, AbyU_DM and SeMet labeled AbyU_DM from a Superdex 75 10/300 column (GE Healthcare) pre-equilibrated in 20 mM Tris-HCl, 150 mM NaCl, pH 7.5. 0.2 mg of each protein was loaded onto the column. Eluted peaks were observed by monitoring the absorbance of the column eluent at 280 nm. Inset, SDS-PAGE analysis of AbyU, AbyU_DM and SeMet labeled AbyU_DM. **B**, Comparative analysis of the elution volumes of AbyU, AbyU_DM and SeMet labeled AbyU_DM with those of Bio-Rad protein standards (thyroglobulin, 670 kDa; γ-globulin, 158 kDa; ovalbumin, 44 kDa; myoglobin, 17 kDa; vitamin B_{12} 1.35 kDa). Protein standards were analyzed using the same column and buffer conditions as those used for AbyU proteins. The theoretically calculated molecular mass of an AbyU dimer, based on amino acid composition, is 36 kDa including vector encoded His-tag and linker.

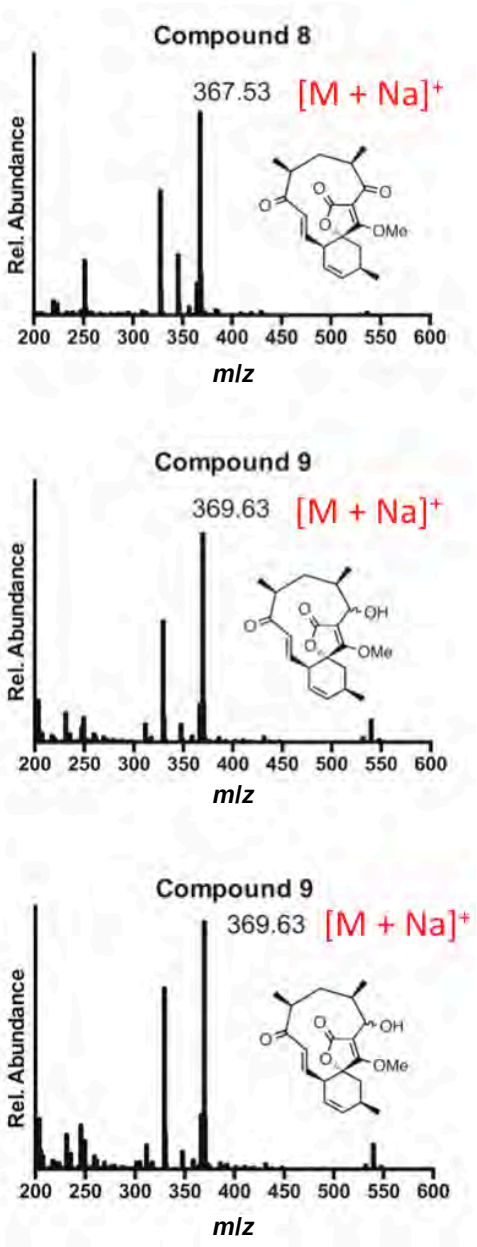

Fig. S2. Mass spectra of AbyU catalyzed reaction products. Positive ion mode ESI MS of **8** and both C3 epimers of product **9** recovered from AbyU catalyzed [4+2] cycloaddition reactions (see fig. 2). Product masses are consistent with the proposed structures of both **8** with *m/z* of $[M + Na]^+$ = 367.53 (theoretically predicted: 367.15), and **9** $[M + Na]^+$ = 369.63 (theoretically predicted: 369.17).

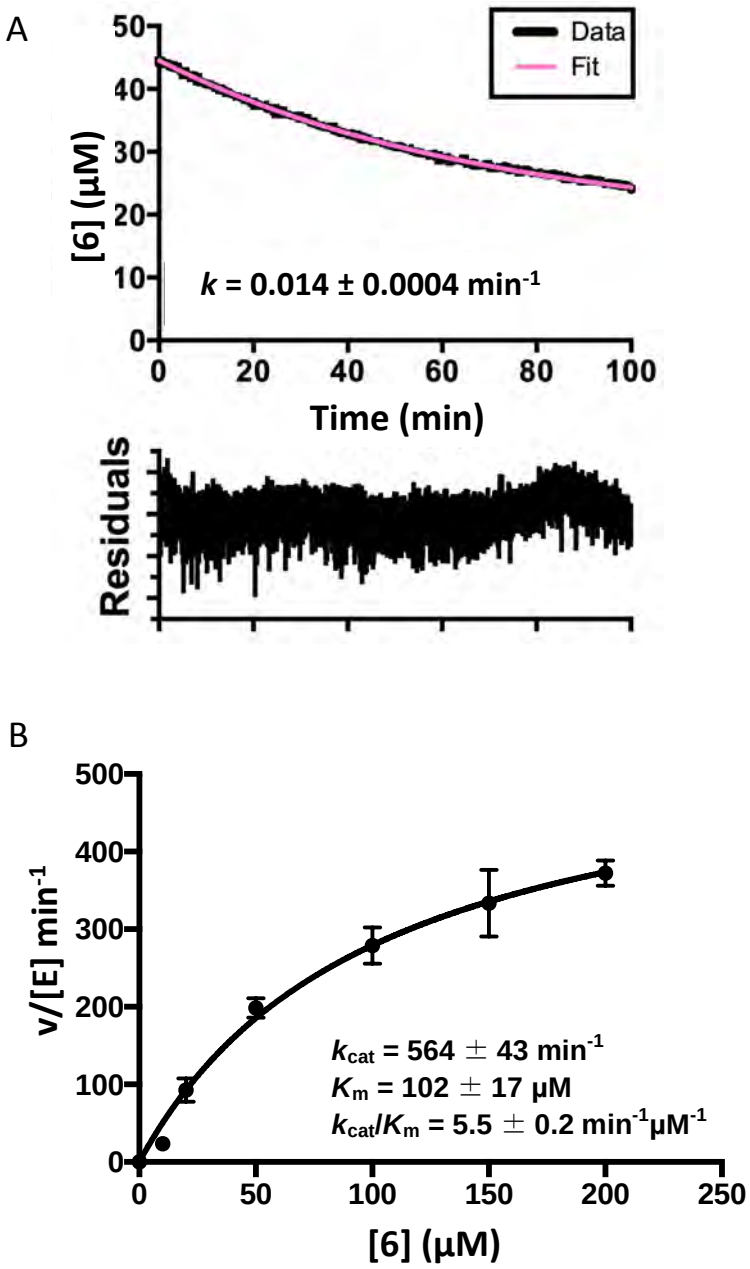

Fig. S3. Kinetic characterization of the non-enzymatically catalyzed and AbyU catalyzed conversion of 6 to 8. A, spontaneous conversion of **6** to **8** monitored spectrophotometrically. Data are fitted to a single exponential as detailed in SI methods. **B**, plot of initial velocity/[E] *vs*. substrate concentration for the AbyU catalyzed conversion of **6** to **8**. Data are fitted to a rectangular hyperbola as detailed in SI methods. Values for initial rates are mean values calculated from three repeats of each experiment. Error bars are standard errors from the mean.

ATG ACG GAA CGC CTT GAA ACC CGT CCT CAA GCG CTG CTC ATC AAA GTA CCG
ACT GAG ATC GTG GTG AAA GTC GTG GAT GAC GTG GAT GTC GCT GCA CCA GCC
GTT GGT CAG GTT GGG AAG TTT GAC GAT GAA CTG TAC GAC GAA GCT GGT GCG
CAG ATT GGC ACC TCT TCC GGC AAT TTC CGC ATT GAG TAC GTA CGT CCG ACT
GAT GGA GGC TTG ATG ACC TAC TAT CAG GAG GAT ATC ACC CTG TCG GAT GGC
GTG ATT CAT GCG GAA GGT TGG GCC GAT TTC AAC GAC GTT CGT ACG AGC AAA
TGG GTG TTT TAT CCG GCA ACA GGC GTT TCA GGA CGC TAT CTG GGC TTA ACC
GGG TTT CGC CAA TGG CGT ATG ACG GGT GTC CGG AAA AGT GCC GAA GCG CGC
ATT CTG ATG GGT GAA

Fig. S4. Sequence of the synthetic *abyU_DM* gene used in this study. Codons encoding methionine residues in *abyU_DM* that replace those encoding leucine residues in *abyU* are highlighted in yellow. Codon optimization was performed by the commercial supplier MWG Eurofins™.

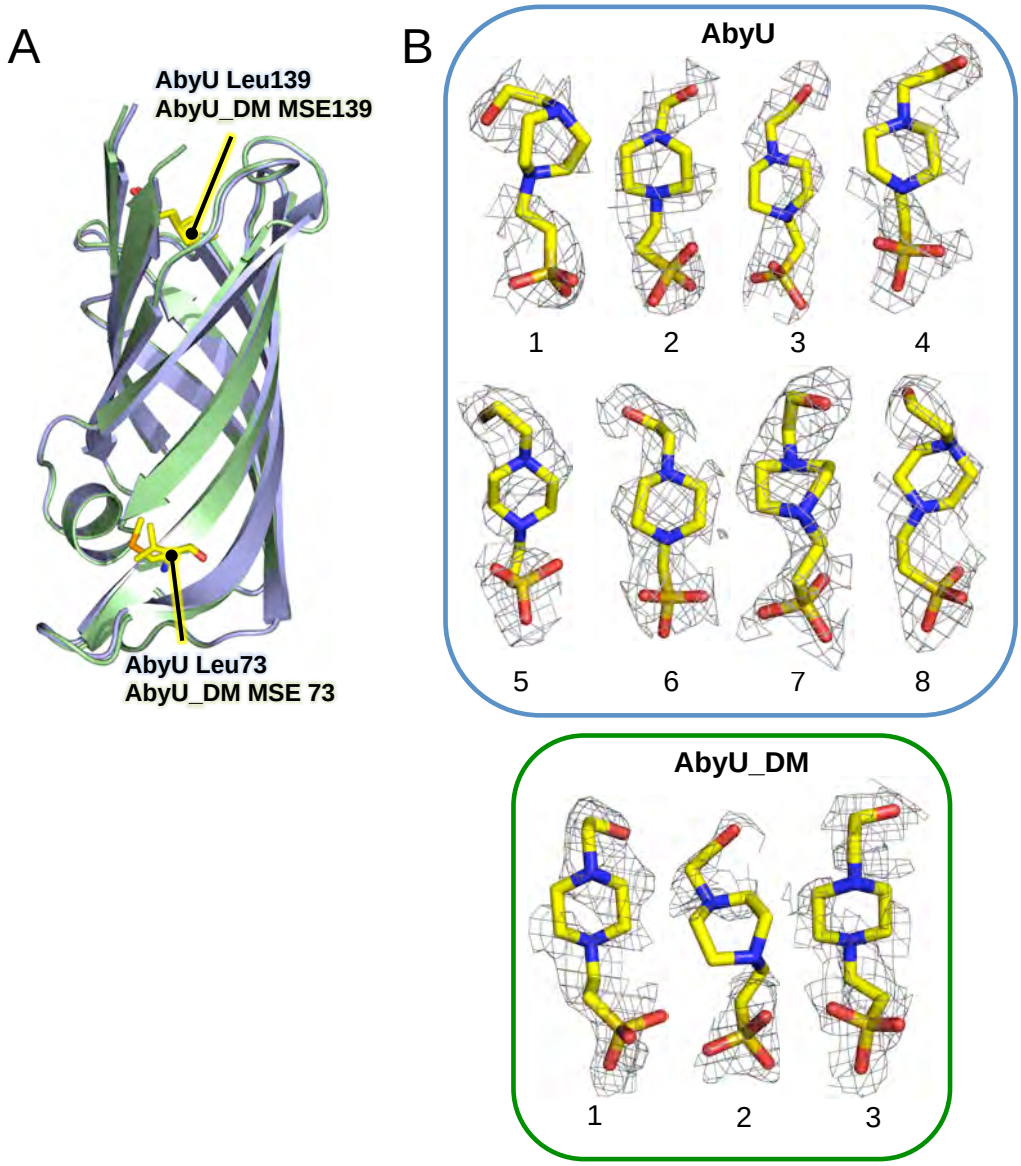

Fig. S5. Structural comparison of AbyU with SeMet labeled AbyU_DM. A, Superposition of the crystal structures of AbyU (blue) and AbyU_DM (green) highlighting the location of the residues 73 and 139. The calculated RMSD between the two structures is 0.4 Å. **B,** $2F_{obs}$-F_{calc} simulated annealing omit maps (gray mesh) contoured at 1.0 σ of HEPES molecules identified in the active sites of each of the 8 copies of AbyU that comprise the asymmetric unit of the AbyU protein crystal, and 3 of the 4 copies of AbyU_DM that comprise the asymmetric unit of the AbyU_DM protein crystal. Ligands are shown in stick representation and colored by atom.

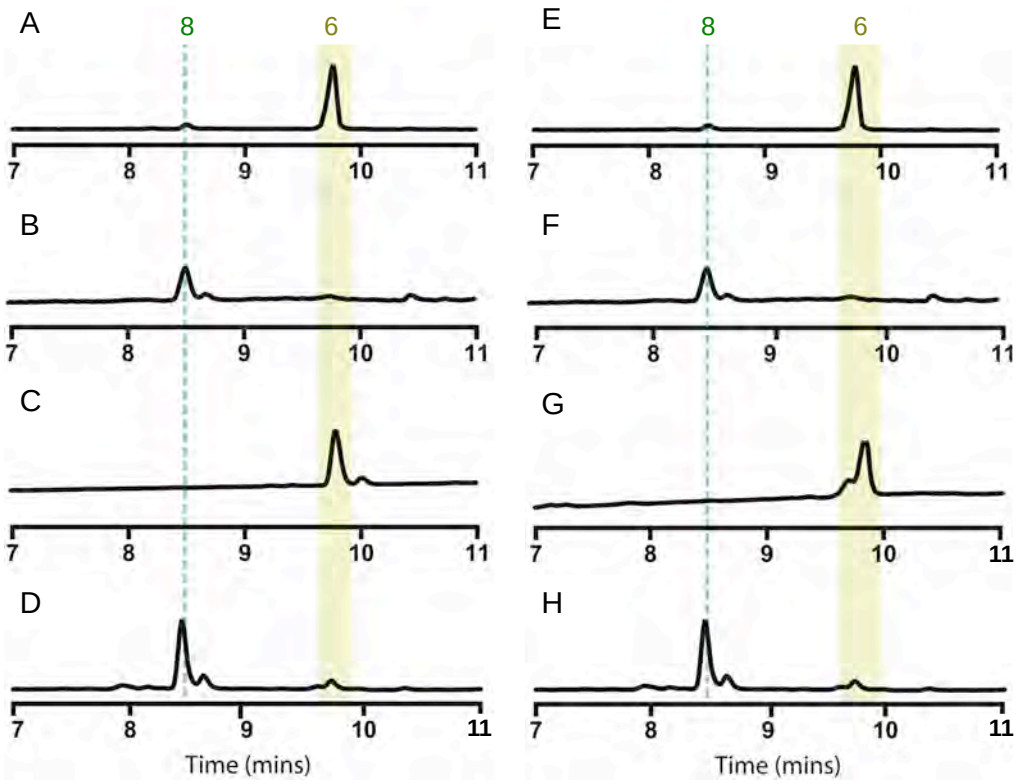

Fig. S6. HPLC analysis demonstrating the ability of unlabeled and SeMet labeled AbyU_DM to catalyze [4+2] cycloaddition. HPLC analysis of reaction mixtures comprising: **A**, 10 mM **6**; **B**, **6** incubated for 30 minutes at 25 °C with 280 μM unlabeled AbyU_DM; **C**, **6** incubated for 30 minutes at 25 °C with 280 μM denatured unlabeled AbyU_DM; **D**, **8** generated using a synthetic Diels-Alder reaction; **E**, 10 mM **6**; **F**, **6** incubated for 30 minutes at 25 °C with 280 μM SeMet labeled AbyU_DM; **G**, **6** incubated for 30 minutes at 25 °C with 280 μM denatured SeMet labeled AbyU_DM; **H**, **8** generated using a synthetic Diels-Alder reaction.

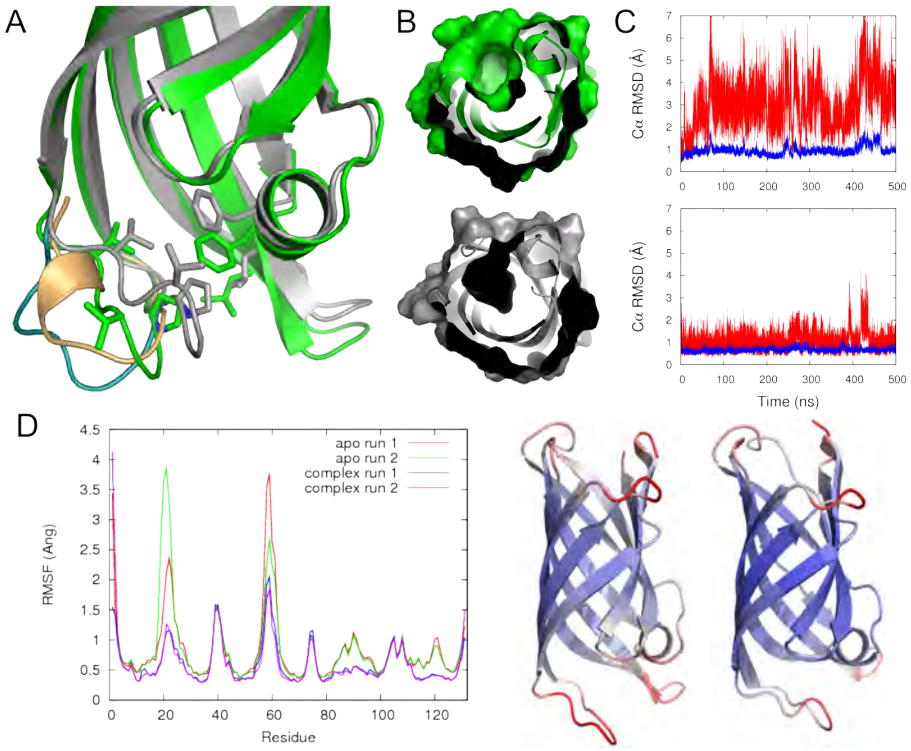

Fig. S7. Flexibility and active site access in AbyU. A, Representative conformations from molecular dynamics (MD) simulations of the loop covering the active site cavity (residues 26-36), obtained by clustering analysis (see SI methods). In gray: the crystal structure (with HEPES removed); in green: a snapshot from simulation of the *apo* form representing 80% of the conformations sampled from 100-500 ns in 4 independent simulations; in light orange and blue: residues 26-36 of snapshots representing 10% and 8% of the conformations sampled, respectively. The main residues forming hydrophobic contacts that can hold the loop closed (V28, V30, P31, L72 and F95) are shown as sticks for the closed starting conformation (gray) and the main open conformation (green). **B**, Entrance to the active site cavity in the closed starting conformation (gray) and the main open conformation (green). **C**, Difference in loop structure and movement in the *apo* and complexed simulations. Cα root-mean square deviations (RMSD) in two representative MD simulations of the apo form (top) and the product **5** bound form (precursor of abyssomycin C; starting complex obtained from docking, see section S4). Blue line depicts the RMSD of the residues making up the strands of the β-barrel, red line depicts the RMSD of the loop residues (26-36) after alignment on the barrel strands. **D**, Flexibility measured by root-mean-square fluctuation (from 50-500 ns) for two independent simulations of the *apo* protein and the protein complexed with product **5**. The average RMSF of the two runs is also projected on representative structures ranging from blue (0 Å) to white to red (1.5 Å and higher); *apo* structure on the right, complex structure on the left. Structural elements that interact with the flexible loop in the closed structure show less flexibility when the loop stays closed.

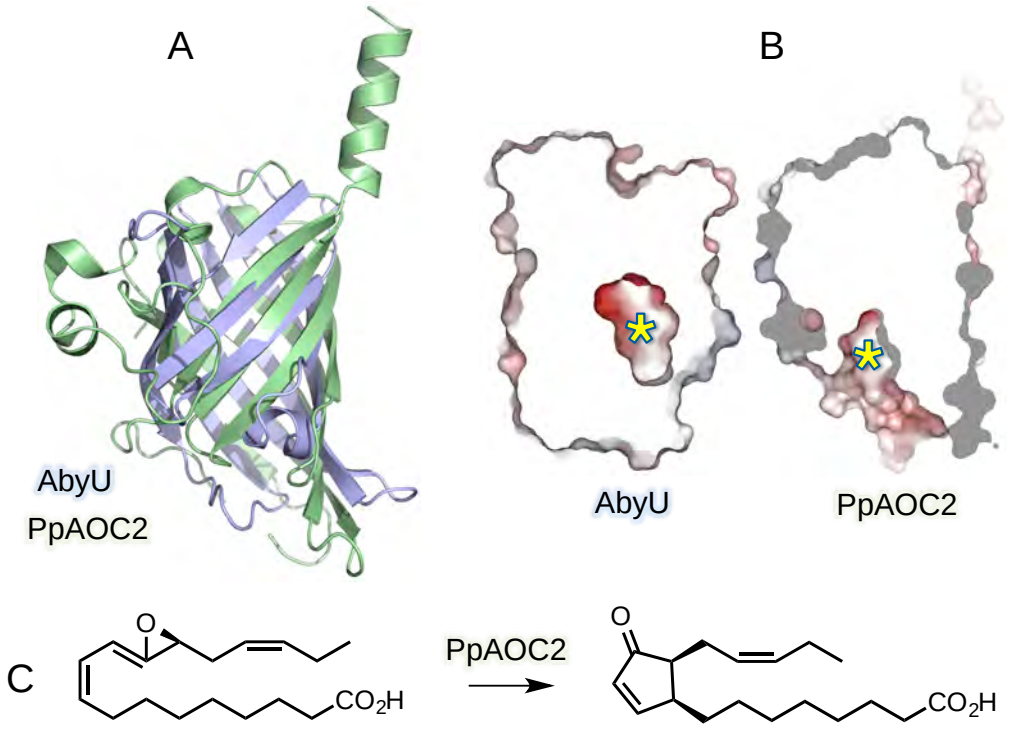

Fig. S8. Structural comparison of AbyU with the allene oxide cyclase pPAOC2. A, Superposition of AbyU (Blue) with pPAOC2 (Green). Both proteins are shown in cartoon representation. **B**, Comparison of the size, shape and location of the active sites of AbyU and pPAOC2. Both proteins are shown in space filling representation and are colored by electrostatic surface potential. The location of the active sites of AbyU and pPAOC2 are indicated by yellow asterisks. **C**, pPAOC2 catalyzed cyclization of the allene oxide 12,13-(*S*)-epoxy-9*Z*,11*E*,15*Z*-octadecatrienoic acid.[31]

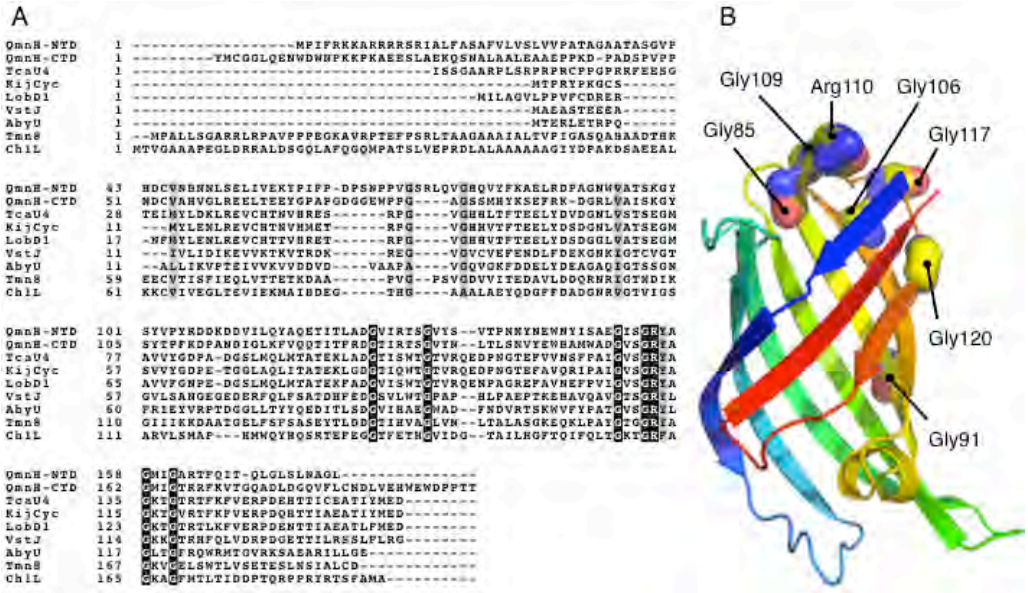

Fig. S9. Amino acid conservation in spirotetronate cyclases and structural implications. A, Comparative sequence alignment of AbyU with other spirotetronate cyclases. Included are QmnH-NTD (quartromicin, N-terminal domain of QmnH), QmnH-CTD (quartromicin, *C*-terminal domain of QmnH), TcaU4 (tetrocarcin), KijCyc (kijanimicin), LobD1 (lobophorines), VstJ (versipelostatin), AbyU (abyssomicins), Tmn8 (tetronomycin), and ChlL (chlorothricin). Amino acids conserved in all the spirotetronate cyclases included in this analysis are highlighted in black boxes. Sequence alignments were performed using ClustalW2.[32] The figure was generated using BOXSHADE (http://www.ch.embnet.org/software/BOX_form.html). **B**, Conserved amino acids identified in (**A**) mapped onto the crystal structure of AbyU. AbyU is shown in cartoon representation colored blue to red from N-terminus to *C*-terminus. Conserved amino acids are show in sphere representation and colored by atom. None of the conserved amino acids are located within the AbyU active site.

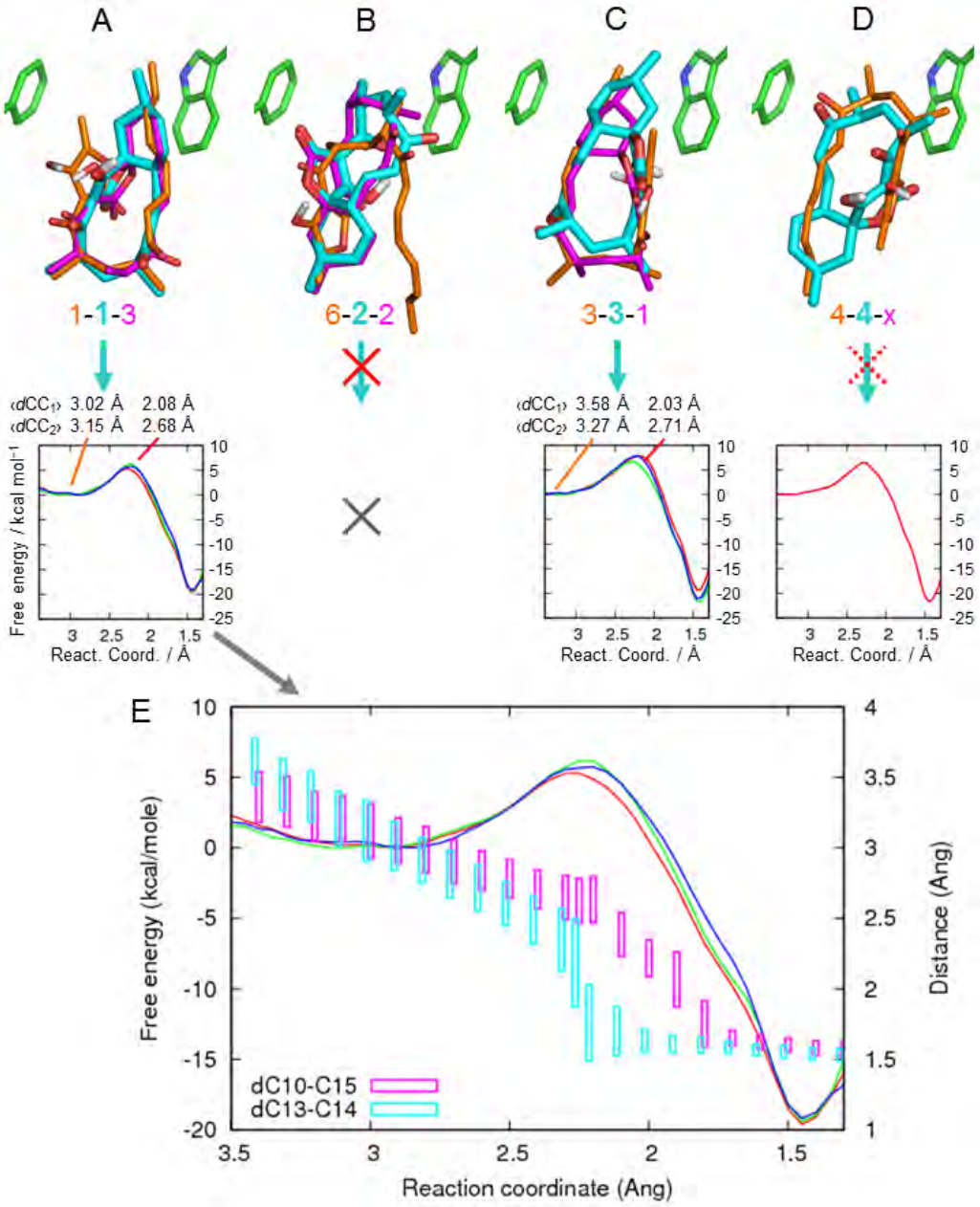

Fig. S10. Docking and QM/MM simulations of substrate and products in AbyU. Top half of panels **A**-**D** represent all 4 different docking poses of the AbyU product **5** (abyssomycin C without the ether-bridge, cyan carbons), together with the equivalent poses of the docked substrate (orange carbons) and the atropisomer product (magenta carbons). AbyU residues Phe41 and Trp124 are indicated for reference (green carbons). Docking ranks are indicated below. Bottom half of panels **A**-**D** indicate the results of QM/MM reaction simulations (starting from the docked product pose), if applicable. Free energies (as obtained from

QM/MM umbrella sampling simulations; see section S4.3 for details) are shown relative to the substrate minimum. Average distances of the forming carbon-carbon bonds (dCC_1 = *d*C13-C14; dCC_2 = dC10-C15) from the sampling windows representing the substrate minimum and the transition state maximum are indicated. These values show that an asynchronous concerted mechanism is followed, with formation of the C13-C14 bond occurring first (and representing the reaction barrier). For the pose in panel **B**, no relevant reactive pathways could be obtained and for the pose in panel **D** only a single reactive pathway. The pose in panel **A** is favored by docking (consistent binding modes of substrate and products) and QM/MM simulation (reactive pathways with the lowest average free energy barrier and a clear substrate minimum). **E**, QM/MM free energy profiles (PMFs) of panel A in more detail. Average distances (+/− standard deviation) of the forming carbon-carbon bonds are indicated (confirming the asynchronous concerted mechanism).

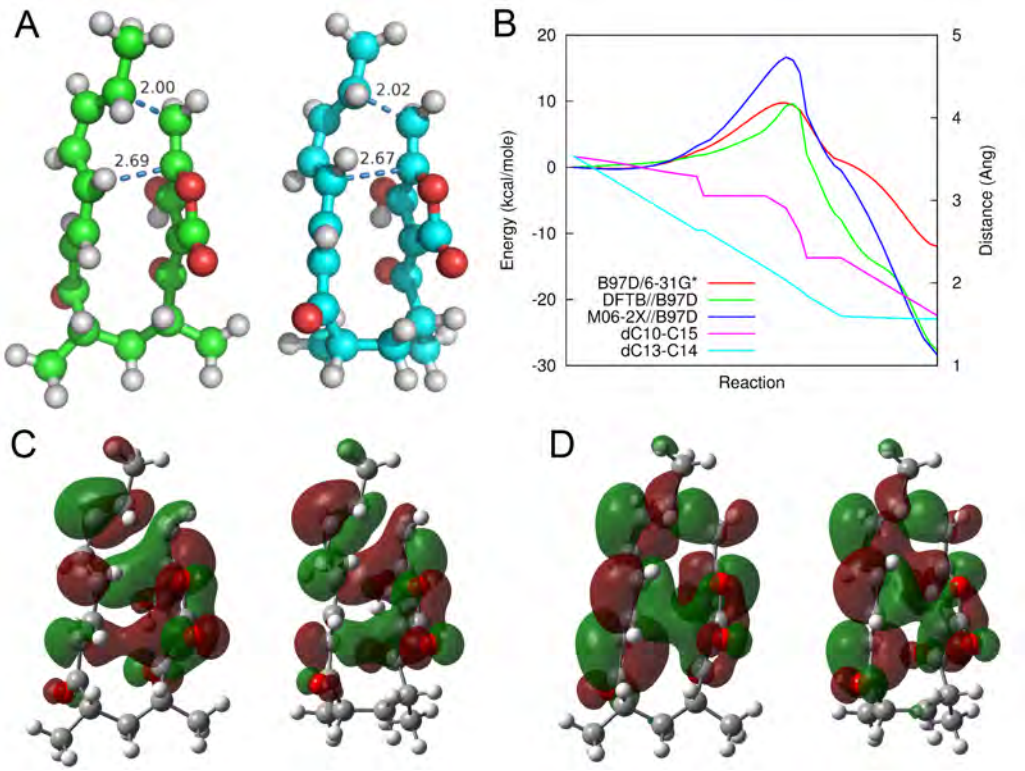

Fig. S11. Transition states for the Diels-Alder reaction. Transition states were optimized in the gas-phase at the M06-2X/6-31G* level for the products of AbyU (see SI methods). **A**, Transition states of product **5** (abyssomycin C without the ether-bridge; green carbons, left) and its atropisomer (cyan carbons, right). The bond distances (indicated by blue dashed lines with distances in A) and single imaginary frequencies indicate that the reaction is asynchronous, with the bond formation between C13 and C14 occurring first. **B**, Approximate potential energy surface for the reaction, starting from the product, obtained by following the minimum energy path in B97D/6-31G* optimizations where either *d*C10-C15 or *d*C13-C14 is increased (see SI methods). Single-point calculations using M06-2X/6-31G* (more accurate) or (SCC-)DFTB (more approximate), indicating that the overall shape between these levels of theory is similar, with (SCC-)DFTB underestimating the reaction barrier by ~7.3 kcal mol^{-1}. **C** & **D**, Depictions of the highest occupied (C) and lowest unoccupied (D) molecular orbitals (HOMO & LUMO) of the transition states (isovalue is 0.02 $electrons^2/bohr^6$); product **5** left, atropisomer of **5** right.

	AbyU_DM	AbyU
Data collection		
Space group	$P2_12_12_1$	$P1$
Cell dimensions		
a, *b*, *c* (Å)	67.35, 68.27, 139.31	61.80, 73.59, 86.19
α, β, γ (°)	90, 90, 90	112.87, 90.04, 89.98
Wavelength (Å)	0.91731	0.97298
Resolution (Å)	29.78–1.77 (1.77-1.72)	79.41-2.36 (2.49-2.36)
R_{merge} (%)	0.106 (0.764)	0.12 (0.358)
$I/\sigma I$	27.8 (3.5)	6.4 (3.27)
Completeness (%)	99.7 (95.9)	92.4 (73.7)
Redundancy	24.1 (16.6)	3.3 (3.2)
Refinement		
Resolution (Å)	29.78-1.77	79.41-2.36
No. reflections	65871	52922
R_{work}/R_{free}	20.1/22.1	20.9/25.0
No. atoms	4203	8472
Protein	4061	8251
Ligand	45	150
Water	97	76
B-factors		
Protein	21.03	22.81
Ligand	39.72	26.16
Water	23.07	17.42
Occupancies		
HEPES	1	1
R.m.s. deviations		
Bond lengths (Å)	0.008	0.007
Bond angles (°)	1.189	1.036

Table S1. X-ray diffraction data collection, phasing and refinement statistics. Data in parentheses correspond to values for the highest resolution shell.

References

(1) Berrow, N. S.; Alderton, D.; Sainsbury, S.; Nettleship, J.; Assenberg, R.; Rahman, N.; Stuart, D. I.; Owens, R. J. *Nucleic Acids Res.* **2007**, *35* (6), e45.

(2) Battye, T. G. G.; Kontogiannis, L.; Johnson, O.; Powell, H. R.; Leslie, A. G. W. *Acta Crystallogr. Sect. D Biol. Crystallogr.* **2011**, *67* (4), 271–281.

(3) Evans, P. R.; Murshudov, G. N. *Acta Crystallogr. D. Biol. Crystallogr.* **2013**, *69* (Pt 7), 1204–1214.

(4) Potterton, E.; Briggs, P.; Turkenburg, M.; Dodson, E. *Acta Crystallogr. - Sect. D Biol. Crystallogr.* **2003**, *59* (7), 1131–1137.

(5) Sheldrick, G. M. *Acta Crystallographica Section A: Foundations of Crystallography*. 2007, pp 112–122.

(6) Terwilliger, T. C.; Grosse-Kunstleve, R. W.; Afonine, P. V.; Moriarty, N. W.; Zwart, P. H.; Hung, L. W.; Read, R. J.; Adams, P. D. In *Acta Crystallographica Section D: Biological Crystallography*; 2007; Vol. 64, pp 61–69.

(7) Perrakis, A.; Morris, R.; Lamzin, V. S. *Nat. Struct. Biol.* **1999**, *6* (5), 458–463.

(8) Emsley, P.; Cowtan, K. *Acta Crystallogr. Sect. D Biol. Crystallogr.* **2004**, *60* (12 I), 2126–2132.

(9) Murshudov, G. N.; Skubák, P.; Lebedev, A. A.; Pannu, N. S.; Steiner, R. A.; Nicholls, R. A.; Winn, M. D.; Long, F.; Vagin, A. A. *Acta Crystallogr. Sect. D Biol. Crystallogr.* **2011**, *67* (4), 355–367.

(10) McCoy, A. J.; Grosse-Kunstleve, R. W.; Adams, P. D.; Winn, M. D.; Storoni, L. C.; Read, R. J. *J. Appl. Crystallogr.* **2007**, *40* (4), 658–674.

(11) DeLano, W. *CCP4 Newsl. Protein Crystallogr.* **2002**.

(12) Trott, O.; Olson, A. J. *J. Comput. Chem.* **2010**, *31* (2), 455–461.

(13) Sondergaard, C. R.; Olsson, M. H. M.; Rostkowski, M.; Jensen, J. H. *J. Chem. Theory Comput.* **2011**, *7* (7), 2284–2295.

(14) Olsson, M. H. M.; Sondergaard, C. R.; Rostkowski, M.; Jensen, J. H. *J. Chem. Theory Comput.* **2011**, *7* (2), 525–537.

(15) Salomon-Ferrer, R.; Götz, A. W.; Poole, D.; Le Grand, S.; Walker, R. C. *J. Chem. Theory Comput.* **2013**, *9* (9), 3878–3888.

(16) Maier, J. A.; Martinez, C.; Kasavajhala, K.; Wickstrom, L.; Hauser, K. E.; Simmerling, C. *J. Chem. Theory Comput.* **2015**, *11* (8), 3696–3713.

(17) Wang, J. M.; Wolf, R. M.; Caldwell, J. W.; Kollman, P. A.; Case, D. A. *J. Comput. Chem.* **2004**, *25* (9), 1157–1174.

(18) Vanquelef, E.; Simon, S.; Marquant, G.; Garcia, E.; Klimerak, G.; Delepine, J. C.; Cieplak, P.; Dupradeau, F.-Y. *Nucleic Acids Res.* **2011**, *39* (suppl 2), W511–W517.

(19) Elstner, M.; Porezag, D.; Jungnickel, G.; Elsner, J.; Haugk, M.; Frauenheim, T.; Suhai, S.; Seifert, G. *Phys. Rev. B* **1998**, *58* (11), 7260–7268.

(20) Zhao, Y.; Schultz, N. E.; Truhlar, D. G. *J. Chem. Phys.* **2005**, *123* (16).

(21) Zhao, Y.; Schultz, N. E.; Truhlar, D. G. *J. Chem. Theory Comput.* **2006**, *2* (2), 364–382.

(22) Zhao, Y.; Truhlar, D. G. *Theor. Chem. Acc.* **2008**, *120* (1-3), 215–241.

(23) Peng, C.; Ayala, P. Y.; Schlegel, H. B.; Frisch, M. J. *J. Comput. Chem.* **1996**, *17* (1), 49–56.

(24) Frisch, M. J.; Trucks, G. W.; Schlegel, H. B.; Scuseria, G. E.; Robb, M. A.; Cheeseman, J. R.; Scalmani, G.; Barone, V.; Mennucci, B.; Petersson, G. A.; Nakatsuji, H.; Caricato, M.; Li, X.; Hratchian, H. P.; Izmaylov, A. F.; Bloino, J.; Zheng, G.; Sonnenberg, J. L.; Hada, M.; Ehara, M.; Toyota, K.; Fukuda, R.; Hasegawa, J.; Ishida, M.; Nakajima, T.; Honda, Y.; Kitao, O.; Nakai, H.; Vreven, T.; Montgomery Jr., J. A.; Peralta, J. E.; Ogliaro, F.; Bearpark, M. J.; Heyd, J.; Brothers, E. N.; Kudin, K. N.; Staroverov, V. N.; Kobayashi, R.; Normand, J.; Raghavachari, K.; Rendell, A. P.; Burant, J. C.; Iyengar, S. S.; Tomasi, J.; Cossi, M.; Rega, N.; Millam, N. J.; Klene, M.; Knox, J. E.; Cross, J. B.; Bakken, V.; Adamo, C.; Jaramillo, J.; Gomperts, R.; Stratmann, R. E.; Yazyev, O.; Austin, A. J.; Cammi, R.; Pomelli, C.; Ochterski, J. W.; Martin, R. L.; Morokuma, K.; Zakrzewski, V. G.; Voth, G. A.; Salvador, P.; Dannenberg, J. J.; Dapprich, S.; Daniels, A. D.; Farkas, Ö.; Foresman, J. B.; Ortiz, J. V; Cioslowski, J.; Fox, D. J. Gaussian, Inc.: Wallingford, CT, USA 2009.

(25) Pieniazek, S. N.; Clemente, F. R.; Houk, K. N. *Angew. Chemie-International Ed.* **2008**, *47* (40), 7746–7749.

(26) Baker, N. A.; Sept, D.; Joseph, S.; Holst, M. J.; McCammon, J. A. *Proc. Natl. Acad. Sci. U.S.A.* **2001**, *98* (18), 10037-10041.

(27) Andrus, M. B.; Li, W.; Keyes, R. F. *J. Org. Chem.* **1997**, *62* (16), 5542-5549.

(28) Montgomery, J.; Challis, G. L. *Synlett* **2008**, *14*, 2164-2168.

(29) Takeda, K.; Yano, S.; Sato, M.; Yoshii, E. *J. Org. Chem.* **1987**, *52* (18), 4135-4137.

(30) Snider, B. B.; Zou, Y. *Org. Lett.* **2005**, *7* (22), 4939-4941.

(31) Neumann, P.; Brodhun, F.; Sauer, K.; Herrfurth, C.; Hamberg, M.; Brinkmann, J.; Scholz, J.; Dickmanns, a.; Feussner, I.; Ficner, R. *Plant Physiol.* **2012**, *160* (3), 1251–1266.

(32) Larkin, M.; Blackshields, G.; Brown, N.; Chenna, R.; McGettigan, P.; McWilliam, H.; Valentin, F.; Wallace, I.; Wilm, A.; Lopez, R.; Thompson, J.; Gibson, T.; Higgins, D. *Bioinformatics* **2007**, *23* (21), 2947–2948.